Conclusion

Using a model analysis, we have shown that the beneficial effect of 1.5VR depends on the RV stiffness constant. 1.5VR is the most beneficial for hypoplastic RV with 150–250% of normal RV stiffness constant. The beneficial range of 1.5VR may also be changed by individual parameters other than the RV stiffness constant, but the beneficial range certainly exists. Therefore, determination of management strategy should be based not only on the morphologic parameters but also on the physiologically determined properties.

Acknowledgments This study was supported by Health and Labor Sciences Research Grants (H18-nano-Ippan-003, H19-nano-Ippan-009, H20-katsudo-Shitei-007 and H21-nano-Ippan-005) from the Ministry of Health, Labor and Welfare of Japan, by Grants-in-Aid for Scientific Research (No. 20390462) from the Ministry of Education, Culture, Sports, Science and Technology in Japan, and by the Industrial Technology Research Grant Program from New Energy and Industrial Technology Development Organization (NEDO) of Japan.

References

1. Yoshimura N, Yamaguchi M, Ohashi H, Oshima Y, Oka S, Yoshida M, Murakami H, Tei T (2003) Pulmonary atresia with intact ventricular septum: strategy based on right ventricular morphology. J Thorac Cardiovasc Surg 126:1417–1426
2. Chowdhury UK, Airan B, Talwar S, Kothari SS, Saxena A, Singh R, Subramaniam GK, Juneja R, Pradeep KK, Sathia S, Venugopal P (2005) One and one-half ventricle repair: results and concerns. Ann Thorac Surg 80:2293–2300
3. Hanley FL (1999) The one and a half ventricle repair-we can do it, but should we do it? J Thorac Cardiovasc Surg 117:659–661
4. Uemura H, Yagihara T, Adachi I, Kagisaki K, Shikata F (2007) Conversion to total cavopulmonary connection after failed one and one-half ventricular repair. Ann Thorac Surg 84:666–668
5. Numata S, Uemura H, Yagihara T, Kagisaki K, Takahashi M, Ohuchi H (2003) Long-term functional results of the one and one half ventricular repair for the spectrum of patients with pulmonary atresia/stenosis with intact ventricular septum. Eur J Cardiothorac Surg 24:516–520
6. Freedom RM (1998) Pulmonary atresia with intact ventricular septum—the significance of the coronary arterial circulation. In: Redington AN, Brawn WJ, Deanfield JE, Anderson RH (eds) The right heart in congenital heart disease. Greenwich Medical Media, London
7. Hanley FL, Sade RM, Blackstone EH, Kirklin JW, Freedom RM, Nanda NC (1993) Outcomes in neonatal pulmonary atresia with intact ventricular septum. A multiinstitutional study. J Thorac Cardiovasc Surg 105:406–427
8. Ashburn DA, Blackstone EH, Wells WJ, Jonas RA, Pigula FA, Manning PB, Lofland GK, Williams WG, McCrindle BW, Congenital Heart Surgeons Study members (2004) Determinants of mortality and type of repair in neonates with pulmonary atresia and intact ventricular septum. J Thorac Cardiovasc Surg 127:1000–1007
9. Burkhoff D, Tyberg JV (1993) Why does pulmonary venous pressure rise after onset of LV dysfunction: a theoretical analysis. Am J Physiol 265:H1819–H1828
10. Morley D, Litwak K, Ferber P, Spence P, Dowling R, Meyns B, Griffith B, Burkhoff D (2007) Hemodynamic effects of partial ventricular support in chronic heart failure: results of simulation validated with in vivo data. J Thorac Cardiovasc Surg 133:21–28
11. Goodwin JA, van Meurs WL, Sá Couto CD, Beneken JE, Graves SA (2004) A model for educational simulation of infant cardiovascular physiology. Anesth Analg 99:1655–1664
12. Migliavacca F, Pennati G, Dubini G, Fumero R, Pietrabissa R, Urcelay G, Bove EL, Hsia TY, de Leval MR (2001) Modeling of the Norwood circulation: effects of shunt size, vascular resistances, and heart rate. Am J Physiol Heart Circ Physiol 280:H2076–H2086
13. Santamore WP, Burkhoff D (1991) Hemodynamic consequences of ventricular interaction as assessed by model analysis. Am J Physiol 260:H146–H157
14. Sagawa K, Maughan L, Suga H, Sunagawa K (1988) Cardiovascular interaction. In: Sagawa K, Maughan L, Suga H, Sunagawa K (eds) Cardiac contraction and the pressure–volume relationship. Oxford University Press, Oxford
15. Walther FJ, Siassi B, King J, Wu PY (1986) Blood flow in the ascending and descending aorta in term newborn infants. Early Hum Dev 13:21–25
16. Wang JJ, Flewitt JA, Shrive NG, Parker KH, Tyberg JV (2006) Systemic venous circulation. Waves propagating on a windkessel: relation of arterial and venous windkessels to systemic vascular resistance. Am J Physiol Heart Circ Physiol 290:H154–H162
17. McElhinney DB, Reddy VM, Hanley FL, Moore P (1997) Systemic venous collateral channels causing desaturation after bidirectional cavopulmonary anastomosis: evaluation and management. J Am Coll Cardiol 30:817–824
18. Gatzoulis MA, Shinebourne EA, Redington AN, Rigby ML, Ho SY, Shore DF (1995) Increasing cyanosis early after cavopulmonary connection caused by abnormal systemic venous channels. Br Heart J 73:182–186
19. Webber SA, Horvath P, LeBlanc JG, Slavik Z, Lamb RK, Monro JL, Reich O, Hruda J, Sandor GG, Keeton BR, Salmon AP (1995) Influence of competitive pulmonary blood flow on the bidirectional superior cavopulmonary shunt. A multi-institutional study. Circulation 92:II279–II286
20. Trusler GA, Williams WG, Cohen AJ, Rabinovitch M, Moes CA, Smallhorn JF, Coles JG, Lightfoot NE, Freedom RM (1990) William Glenn lecture. The cavopulmonary shunt. Evolution of a concept. Circulation 82:IV131–IV138
21. Gelatt M, Hamilton RM, McCrindle BW, Gow RM, Williams WG, Trusler GA, Freedom RM (1994) Risk factors for atrial tachyarrhythmias after the Fontan operation. J Am Coll Cardiol 24:1735–1741
22. Balaji S, Gewillig M, Bull C, de Leval MR, Deanfield JE (1991) Arrhythmias after the Fontan procedure. Comparison of total cavopulmonary connection and atriopulmonary connection. Circulation 84:III162–III167
23. Little WC, Ohno M, Kitzman DW, Thomas JD, Cheng CP (1995) Determination of left ventricular chamber stiffness from the time for deceleration of early left ventricular filling. Circulation 92:1933–1939
24. Lisauskas JB, Singh J, Bowman AW, Kovács SJ (2001) Chamber properties from transmitral flow: prediction of average and passive left ventricular diastolic stiffness. J Appl Physiol 91:154–162
25. Garcia MJ, Firstenberg MS, Greenberg NL, Smedira N, Rodriguez L, Prior D, Thomas JD (2001) Estimation of left ventricular operating stiffness from Doppler early filling deceleration time in humans. Am J Physiol Heart Circ Physiol 280:H554–H561
26. Gaynor SL, Maniar HS, Bloch JB, Steendijk P, Moon MR (2005) Right atrial and ventricular adaptation to chronic right ventricular pressure overload. Circulation 112:I212–I218
27. Szabó G, Buhmann V, Graf A, Melnitschuk S, Bährle S, Vahl CF, Hagl S (2003) Ventricular energetics after the Fontan operation: contractility-afterload mismatch. J Thorac Cardiovasc Surg 125:1061–1069

Autonomic Neuroscience: Basic and Clinical 152 (2010) 115–118

Contents lists available at ScienceDirect

Autonomic Neuroscience: Basic and Clinical

journal homepage: www.elsevier.com/locate/autneu

Short communication

In vivo direct monitoring of interstitial norepinephrine levels at the sinoatrial node

Shuji Shimizu [a,c,d,*], Tsuyoshi Akiyama [b], Toru Kawada [a], Toshiaki Shishido [a], Masaki Mizuno [a], Atsunori Kamiya [a], Toji Yamazaki [b], Shunji Sano [c], Masaru Sugimachi [a]

[a] Department of Cardiovascular Dynamics, Advanced Medical Engineering Center, National Cardiovascular Center Research Institute, Osaka, Japan
[b] Department of Cardiac Physiology, National Cardiovascular Center Research Institute, Osaka, Japan
[c] Department of Cardiovascular Surgery, Okayama University Graduate School of Medicine, Dentistry and Pharmaceutical Sciences, Okayama, Japan
[d] Japan Association for the Advancement of Medical Equipment, Tokyo, Japan

ARTICLE INFO

Article history:
Received 1 June 2009
Received in revised form 12 August 2009
Accepted 27 August 2009

Keywords:
Heart rate
Sympathetic nerve terminal activity
Norepinephrine
Sinoatrial node
Microdialysis
Desipramine

ABSTRACT

We assessed in vivo interstitial norepinephrine (NE) levels at the sinoatrial node in rabbits, using microdialysis technique. A dialysis probe was implanted adjacent to the sinoatrial node of an anesthetized rabbit and dialysate was sampled during sympathetic nerve stimulation. Atrial dialysate NE concentration correlated well with heart rate. Desipramine significantly increased dialysate NE concentrations both before and during sympathetic nerve stimulation compared with the absence of desipramine. However, desipramine did not affect the relation between heart rate and dialysate NE concentration. These results suggest that atrial dialysate NE level reflects the relative change of NE concentration in the synaptic cleft. Microdialysis is a powerful tool to assess in vivo interstitial NE levels at the sinoatrial node.

1. Introduction

Heart rate is determined by the frequency of depolarization of sinoatrial (SA) nodal cell during sinus rhythm. The SA node is innervated by sympathetic nerve fibers. These sympathetic nerves, together with parasympathetic nerves, play an important role in the regulation of SA node pacemaker activities. Direct measurement of electrical axonal activity of efferent cardiac sympathetic nerve (Kawada et al., 2004) and indirect measurement of norepinephrine (NE) spillover from plasma NE concentration in the coronary sinus (Meredith et al., 1993) have been used as indices of sympathetic nerve terminal activity on the effector, i.e. sinoatrial node. However, due to the heterogeneity of sympathetic innervation in the heart, quantitative assessment of sympathetic nerve terminal activities on the SA node is essential for better understanding of the sympathetic control of heart rate.

Recently we have developed a microdialysis technique that allows direct monitoring of acetylcholine release into the SA node (Shimizu et al., 2009). In the present study, we monitored interstitial NE levels in the right atrial myocardium adjacent to the SA node using the microdialysis technique and investigated the relation between interstitial NE levels and heart rate in response to sympathetic nerve stimulation. This study may prove the usefulness of microdialysis in assessing the relative change of sympathetic nerve terminal activity on the SA mode.

2. Materials and methods

2.1. Surgical preparation

Animal care was provided in accordance with the *Guiding Principles for the Care and Use of Animals in the Field of Physiological Sciences* approved by the Physiological Society of Japan. All protocols were approved by the Animal Subject Committee of the National Cardiovascular Center. Fourteen Japanese white rabbits weighing 2.4 to 2.8 kg were used in this study. Anesthesia was initiated by an intravenous injection of pentobarbital sodium (50 mg/kg) via the marginal ear vein, and then maintained at an appropriate level by continuous intravenous infusion of α-chloralose and urethane (16 mg/kg/h and 100 mg/kg/h) through a catheter inserted into the femoral vein. The animals were intubated and ventilated mechanically with room air mixed with oxygen. Systemic arterial pressure was monitored by a catheter inserted into the femoral artery. Esophageal temperature, which was measured by a thermometer (CTM-303, Terumo, Japan), was maintained between 38 and 39 °C using a heating pad. Bilateral vagal nerves were exposed through a midline cervical incision and sectioned at the neck.

With the animal in supine position, a full median sternotomy was performed to expose the heart. The right cardiac sympathetic nerve

* Corresponding author. Department of Cardiovascular Dynamics, Advanced Medical Engineering Center, National Cardiovascular Center Research Institute, 5-7-1, Fujishiro-dai, Suita, Osaka, 565-8565, Japan. Tel.: +81 6 6833 5012; fax: +81 6 6835 5403.
E-mail address: shujismz@ri.ncvc.go.jp (S. Shimizu).

1566-0702/$ – see front matter © 2009 Elsevier B.V. All rights reserved.
doi:10.1016/j.autneu.2009.08.017

was exposed through the sternotomy and sectioned intrathoracically. A pair of bipolar stainless steel electrodes was attached to the efferent side of the right cardiac sympathetic nerve. The nerve and electrode were immobilized using a quick-dry silicone gel (Kwik-Cast and Kwik-Sil, World Precision Instruments, Inc., FL, USA). When sympathetic stimulation was required, the efferent sympathetic nerve was stimulated by a digital stimulator (SEN-7203, Nihon Kohden, Japan), at a pulse duration of 1 ms and an amplitude of 5 V. Three stainless electrodes were attached around the incision of sternotomy for the body surface electrocardiogram. The heart rate was determined from the electrocardiogram using a cardiotachometer. Heparin sodium (100 IU/kg) was administered intravenously to prevent blood coagulation. A dialysis probe was implanted and dialysis was conducted as described in *Dialysis Technique* below. At the end of the experiment, the animal was euthanized with an overdose injection of pentobarbital sodium. In the postmortem examination, the right atrial wall was resected with dialysis fiber. We observed the inside of atrial wall macroscopically and confirmed that the dialysis membrane was not exposed to right atrial lumen.

2.2. Dialysis technique

The materials and properties of the dialysis probe have been described previously. (Akiyama et al., 1991; Shimizu et al., 2009) A dialysis fiber of semipermeable membrane (4 mm length, 310 μm outer diameter, 200 μm inner diameter; PAN-1200, 50,000 molecular weight cutoff; Asahi Chemical, Tokyo, Japan) was attached at both ends to polyethylene tubes (25 cm length, 500 μm outer diameter, 200 μm inner diameter). A fine guiding needle (30 mm length, 510 μm outer diameter, 250 μm inner diameter) with a stainless steel rod (5 mm length, 250 μm outer diameter) was used for the implantation of the dialysis probe. A dialysis probe was implanted into the right atrial myocardium near the junction between the superior vena cava and the right atrium. After implantation, the dialysis probe was perfused with Ringer's solution (NaCl 147 mM, KCl 4 mM, $CaCl_2$ 3 mM) at a speed of 2 μl/min, using a microinjection pump (CMA/102, Carnegie Medicin, Sweden). Experimental protocols were started 120 min after implantation of the dialysis probe. We took account of the dead space between the dialysis membrane and the sample tube at the start of each dialysate sampling. Four-μl phosphate buffer (pH 3.5) was transferred into each sample tube before dialysate sampling. Dialysate sampling periods were set at 10 min (1 sample volume = 20 μl). Dialysate NE concentration was analyzed by high performance liquid chromatography (Akiyama et al., 1991).

2.3. Experimental protocols

2.3.1. Protocol 1

To examine whether atrial interstitial NE level reflects NE release from cardiac sympathetic nerve endings, we investigated the effect of sympathetic nerve stimulation on dialysate NE concentration and analyzed the relationship between the dialysate NE concentrations and heart rate ($n = 7$). We sampled control dialysate after transecting the right sympathetic nerve. Then we stimulated the right sympathetic nerve for 10 min each at frequencies of 2, 5 and 10 Hz, and collected the dialysate during each stimulation. There was a 30-min interval between the different stimulation frequencies. Twenty min after sympathetic nerve stimulation, we sampled the dialysate again to check for recovery of NE level.

2.3.2. Protocol 2

Most of the released NE is removed by neuronal uptake mechanism in the heart (Goldstein et al., 1988). To examine whether an increase in atrial interstitial NE level reflects the increase in synaptic NE levels associated with inhibition of neuronal uptake, we investigated the effects of sympathetic nerve stimulation on dialysate NE concentration in the presence of neuronal uptake inhibition and analyzed the relationship between dialysate NE concentration and heart rate ($n = 7$). After intravenous administration of a neuronal uptake inhibitor, desipramine (1.0 mg/kg), we stimulated the right sympathetic nerve and sampled the dialysate in a similar fashion as in Protocol 1.

2.4. Statistical analysis

All data are presented as means ± SE. Heart rate and dialysate NE concentrations (logarithmic transformation) in response to sympathetic stimulation were compared between the absence and presence of desipramine by two-way analysis of variance (ANOVA). If there was not a significant interaction between desipramine and stimulation effects, heart rate and dialysate NE concentrations (logarithmic transformation) in response to sympathetic stimulation were compared using Dunnett's test. After logarithmic transformation of dialysate NE concentration, a linear regression analysis was performed to examine the relation between dialysate NE concentration and heart rate. The differences in slope and intercept between two regression lines were examined. (Glantz, 2005) Differences were considered significant at $P < 0.05$.

3. Results

In Protocol 1 (stimulation alone), right cardiac sympathetic nerve stimulation significantly increased heart rate from 260 ± 8 bpm in the pre-stimulation control to 298 ± 11 bpm during stimulation at 2 Hz ($P < 0.01$ vs. control), 319 ± 10 bpm at 5 Hz ($P < 0.01$ vs. control) and 318 ± 11 bpm at 10 Hz ($P < 0.01$ vs. control) (ANOVA, $P < 0.001$). Heart rate recovered to 261 ± 9 bpm 20 min after stimulation. Right cardiac sympathetic nerve stimulation significantly increased dialysate NE concentration from 0.4 ± 0.1 nM in the pre-stimulation control to 1.0 ± 0.1 nM during stimulation at 2 Hz ($P < 0.01$ vs. control), 2.2 ± 0.5 nM at 5 Hz ($P < 0.01$ vs. control) and 2.9 ± 0.9 nM at 10 Hz ($P < 0.01$ vs. control) (ANOVA, $P < 0.001$). Dialysate NE concentration recovered to the pre-stimulation level 20 min after stimulation (0.6 ± 0.1 nM) (Fig. 1).

In Protocol 2 (desipramine + stimulation), intravenous administration of desipramine significantly increased baseline heart rate (295 ± 11 vs. 263 ± 11 bpm, $P < 0.01$, paired t test) and baseline dialysate NE concentration (1.5 ± 0.2 vs. 0.8 ± 0.2 nM, $P < 0.01$, paired t test) compared

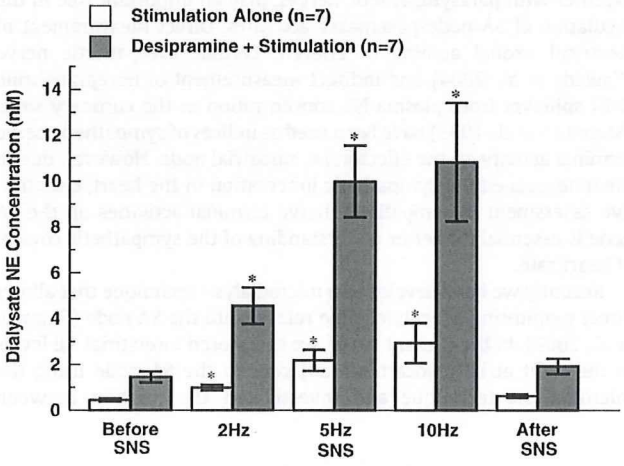

Fig. 1. Dialysate NE concentrations of controls and during electrical stimulation of right cardiac sympathetic nerve at different frequencies. The two-way analysis of variance (ANOVA) revealed the significant effect of sympathetic nerve stimulation on dialysate NE concentration ($P < 0.001$) and the significant difference in dialysate NE concentration ($P < 0.001$) between the absence and presence of desipramine. The interaction between desipramine and stimulation effects was not significant. Values are means ± SE; NE: norepinephrine; SNS: electrical sympathetic nerve stimulation; *n*: number of rabbits; *: $P < 0.01$ vs. the pre-stimulation control by Dunnett's test.

to Protocol 1. Right cardiac sympathetic nerve stimulation significantly increased heart rate from 295 ± 11 bpm in the pre-stimulation control to 349 ± 9 bpm during stimulation at 2 Hz ($P<0.01$ vs. control), 361 ± 8 bpm at 5 Hz ($P<0.01$ vs. control) and 351 ± 9 bpm at 10 Hz ($P<0.01$ vs. control) (ANOVA, $P<0.001$). Heart rate recovered to 295 ± 13 bpm 20 min after stimulation. Right sympathetic nerve stimulation also increased dialysate NE concentration from 1.5 ± 0.2 nM in the pre-stimulation control to 4.6 ± 0.8 nM during stimulation at 2 Hz ($P<0.01$ vs. control), 10.0 ± 1.6 nM at 5 Hz ($P<0.01$ vs. control) and 10.8 ± 2.6 nM at 10 Hz ($P<0.01$ vs. control) (ANOVA, $P<0.001$). Dialysate NE concentration recovered to the pre-stimulation level 20 min after stimulation (1.9 ± 0.3 nM) (Fig. 1). Heart rate and dialysate NE concentrations in Protocol 2 (desipramine + stimulation) were significantly higher than those in Protocol 1 (stimulation alone) (ANOVA, $P<0.001$). The interaction between desipramine and stimulation effects was not significant.

The relation between heart rate and dialysate NE concentration is shown in Fig. 2. Dialysate NE concentration correlated well with heart rate in both Protocols 1 and 2 (Protocol 1: $HR = 290 + 87 \times \log[NE(nM)]$, $R^2 = 0.71$; Protocol 2: $HR = 283 + 74 \times \log[NE(nM)]$, $R^2 = 0.70$) There was no significant difference in the intercept or slope between the two regression lines obtained from Protocols 1 and 2. (Glantz, 2005)

4. Discussion

We were able to monitor in vivo interstitial NE levels at the SA node using microdialysis technique. A neuronal uptake inhibitor, desipramine, significantly increased dialysate NE concentration in the right atrial myocardium. However, desipramine scarcely affected the relation between interstitial NE levels and heart rate.

4.1. Characteristics of dialysate NE concentration in right atrial myocardium

Dialysate NE concentration in the right atrial myocardium increased in response to electrical stimulation of the right cardiac sympathetic nerve and decreased to the pre-stimulation level after stimulation. These results indicate that atrial dialysate NE concentration reflects NE release from cardiac sympathetic nerve endings innervating the right atrium. Furthermore, a semi-log plot demonstrated a linear relationship between the right atrial dialysate NE concentration and heart rate. Judging from this relation, a 10-fold increase in dialysate NE concentration corresponds to an increase in heart rate of 87 bpm. The relative changes in NE release monitored by microdialysis correlate well with the frequency in depolarization of the SA nodal cell. Thus, we consider that dialysate NE concentration does reflect the relative changes in synaptic NE level. The relation between exogenous NE concentration and heart rate has been investigated in the isolated rabbit's atria (Toda, 1969). However, there is no report of a direct method to assess the endogenous NE release into the SA node. Microdialysis enables the monitoring of endogenous NE release into the SA node.

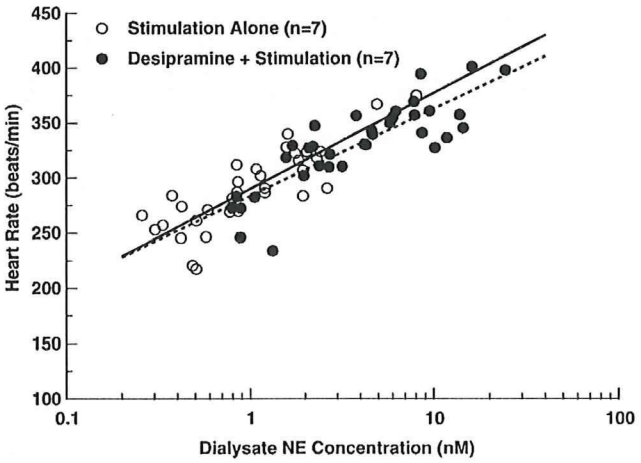

Fig. 2. Relation between dialysate NE concentration (logarithmic scale) and heart rate. Dialysate NE concentration in the right atrial myocardium correlates well with heart rate. Solid line: regression line fitting 35 data points obtained from Protocol 1 (stimulation alone) ($R^2 = 0.71$); dotted line: regression line fitting 35 data points obtained from Protocol 2 (desipramine + stimulation) ($R^2 = 0.70$). NE: norepinephrine.

4.2. Effect of neuronal uptake on dialysate NE concentration

In the presence of desipramine, a neuronal uptake inhibitor, dialysate NE concentration also increased in response to sympathetic nerve stimulation and decreased to the pre-stimulation levels after stimulation. However, dialysate NE concentrations were 3.1–4.6 times higher than the corresponding values in the absence of desipramine. These results are consistent with earlier experimental studies demonstrating that a large part of released NE is removed by neuronal uptake (Goldstein et al., 1988). In the present study, we were able to monitor the change in neuronal NE uptake function induced by desipramine using microdialysis technique.

Linked with the increase in dialysate NE concentrations in the presence of desipramine, heart rates were 33–51 bpm higher than the corresponding values in the absence of desipramine. Thus, desipramine does not alter the relation between dialysate NE concentration and heart rate. The intercept and the slope of regression line also did not differ significantly in the presence and absence of desipramine. These results indicate that neuronal uptake removes effective NE from the synaptic cleft without affecting the sensitivity of the SA nodal cell, and that neuronal NE uptake function plays an important role in the regulation of heart rate. The increase in synaptic NE concentration induced by inhibition of neuronal uptake affects the frequency of depolarization of the SA nodal cell.

Endoh (1975) reported that desipramine shifted the dose–response curve for exogenous NE to the lower NE levels. Since desipramine suppresses the neuronal uptake of both endogenous and exogenous NE, the increase in effective NE on the sinoatrial node may yield this apparent shift in the dose–response curve. Our results suggest that desipramine-inhibited neuronal uptake scarcely affects the relation between synaptic NE concentration and heart rate. Therefore, microdialysis may be a powerful tool to assess the change of synaptic NE concentration in the SA node.

4.3. Limitation

There were several limitations in the present study. First, since we did not section the left cardiac sympathetic nerve, the influence of left sympathetic nerve on the dialysate NE concentration cannot be excluded. Therefore, intravenous administration of desipramine could inhibit neuronal NE uptake at the left sympathetic nerve endings and increase dialysate NE concentration. Second, desipramine may affect the dynamic response of heart rate to sympathetic activation. We have already reported that desipramine decreases the natural frequency of the transfer function from sympathetic nerve activity to heart rate (Kawada et al., 2004). However, cardiac microdialysis using shorter dialysis fiber requires 10-min sampling time to detect changes in myocardial interstitial NE levels. Therefore, we were not able to investigate the dynamic response of heart rate to sympathetic activation in this study.

4.4. Conclusion

We were able to monitor endogenous NE release into the SA node and detect the changes in neuronal uptake function using microdialysis technique. Neuronal NE uptake together with NE release functions play

an important role in the regulation of synaptic NE concentration in the SA node. Microdialysis is a powerful tool to assess the changes of synaptic NE concentration in the SA node.

Acknowledgements

This study was supported by Health and Labor Sciences Research Grants (H18-nano-Ippan-003, H19-nano-Ippan-009, H20-katsudo-Shitei-007 and H21-nano-Ippan-005) from the Ministry of Health, Labor and Welfare of Japan, by Grants-in-Aid for Scientific Research (No. 20390462) from the Ministry of Education, Culture, Sports, Science and Technology in Japan and by the Industrial Technology Research Grant Program from New Energy and Industrial Technology Development Organization (NEDO) of Japan.

References

Akiyama, T., Yamazaki, T., Ninomiya, I., 1991. In vivo monitoring of myocardial interstitial norepinephrine by dialysis technique. Am. J. Physiol. 261, H1643–H1647.

Endoh, M., 1975. Effects of dopamine on sinus rate and ventricular contractile force of the dog heart in vitro and in vivo. Br. J. Pharmacol. 55, 475–486.

Glantz, S.A., 2005. Primer of Biostatistics, 6th ed. McGraw-Hill, New York.

Goldstein, D.S., Brush Jr., J.E., Eisenhofer, G., Stull, R., Esler, M., 1988. In vivo measurement of neuronal uptake of norepinephrine in the human heart. Circulation 78, 41–48.

Kawada, T., Miyamoto, T., Uemura, K., Kashihara, K., Kamiya, A., Sugimachi, M., Sunagawa, K., 2004. Effects of neuronal norepinephrine uptake blockade on baroreflex neural and peripheral arc transfer characteristics. Am. J. Physiol. Regul. Integr. Comp. Physiol. 286, R1110–R1120.

Meredith, I.T., Eisenhofer, G., Lambert, G.W., Dewar, E.M., Jennings, G.L., Esler, M.D., 1993. Cardiac sympathetic nervous activity in congestive heart failure. Evidence for increased neuronal norepinephrine release and preserved neuronal uptake. Circulation 88, 136–145.

Shimizu, S., Akiyama, T., Kawada, T., Shishido, T., Yamazaki, T., Kamiya, A., Mizuno, M., Sano, S., Sugimachi, M., 2009. In vivo direct monitoring of vagal acetylcholine release to the sinoatrial node. Auton. Neurosci. 148, 44–49.

Toda, N., 1969. Interactions of ouabain and noradrenaline in isolated rabbit's atria. Br. J. Pharmacol. 36, 393–408.

Neurochemistry International xxx (2009) xxx–xxx

Contents lists available at ScienceDirect

Neurochemistry International

journal homepage: www.elsevier.com/locate/neuint

Role of Ca^{2+}-activated K^+ channels in catecholamine release from *in vivo* rat adrenal medulla

Tsuyoshi Akiyama [a,*], Toji Yamazaki [a], Toru Kawada [b], Shuji Shimizu [b], Masaru Sugimachi [b], Mikiyasu Shirai [a]

[a] *Department of Cardiac Physiology, National Cardiovascular Center Research Institute, 5-7-1 Fujishiro-dai, Suita, 565-8565 Osaka, Japan*
[b] *Department of Cardiovascular Dynamics, National Cardiovascular Center Research Institute, Suita, 565-8565, Japan*

ARTICLE INFO

Article history:
Received 24 September 2009
Received in revised form 21 October 2009
Accepted 28 October 2009
Available online xxx

Keywords:
Anesthetized rats
Microdialysis technique
Acetylcholine
Norepinephrine
Epinephrine
Ca^{2+}-activated K^+ channels

ABSTRACT

To elucidate the role of Ca^{2+}-activated K^+ (K_{Ca}) channels in the presynaptic acetylcholine (ACh) release from splanchnic nerve endings and the postsynaptic catecholamine release from chromaffin cells, we applied microdialysis technique to the left adrenal medulla of anesthetized rats and investigated the effects of local administration of K_{Ca} channel antagonists through dialysis probes on the release of ACh and/or catecholamine, induced by electrical stimulation of splanchnic nerves or local administration of ACh through the dialysis probes. *Nerve stimulation-induced release*: in the presence of a cholinesterase inhibitor, neostigmine, large-conductance K_{Ca} (BK) channel antagonists, iberiotoxin and paxilline enhanced the presynaptic ACh release and postsynaptic norepinephrine (NE) and epinephrine (Epi) release. Small-conductance K_{Ca} (SK) channel antagonists, apamin and scyllatoxin enhanced the Epi release without any changes in ACh or NE release. In the absence of neostigmine, ACh release was not detected. Iberiotoxin and paxilline enhanced NE and Epi release. Apamin and scyllatoxin had no effect on NE or Epi release. *Exogenous ACh-induced release*: iberiotoxin and paxilline enhanced the Epi release, but had no effect on the NE release. Apamin and scyllatoxin enhanced both NE and Epi release. In conclusion, BK channels on splanchnic nerve endings play an inhibitory role in the physiological catecholamine release from adrenal medulla by limiting presynaptic ACh release while SK channels do not. BK channels on Epi-storing cells may play an inhibitory role in nerve stimulation-induced Epi release. SK channels on NE- and Epi-storing cells play a minor role in nerve stimulation-induced catecholamine release.

1. Introduction

The physiological release of catecholamine from adrenal medulla is controlled by central sympathetic neurons through splanchnic nerves. Splanchnic nerve endings make synaptic-like contacts with chromaffin cells (Coupland, 1965). Activation of splanchnic nerve endings causes Ca^{2+} influx through voltage-dependent Ca^{2+} channels, which evokes exocytotic acetylcholine (ACh) release. This ACh release activates cholinergic receptors on chromaffin cells, which causes Ca^{2+} influx through voltage-dependent Ca^{2+} channels and evokes exocytotic catecholamine release from chromaffin cells (García et al., 2006).

Ca^{2+}-activated K^+ (K_{Ca}) currents are consistently found at neuronal cells or nerve terminals (Meir et al., 1999). K_{Ca} channels are located in the vicinity of voltage-dependent Ca^{2+} channels and activated by Ca^{2+} influx through voltage-dependent Ca^{2+} channels. Activation of the K_{Ca} channels induces outward efflux of K^+, causes hyperpolarization of the membrane, and subsequently limits Ca^{2+} entry through voltage-dependent Ca^{2+}channels. Thus, K_{Ca} channels may be present at two different sites in the adrenal medulla: splanchnic nerve endings and chromaffin cells, and are then involved in the physiological regulation of presynaptic ACh release and/or postsynaptic catecholamine release. In fact, it has been reported that K_{Ca} channels on chromaffin cells play an important role in catecholamine release (Montiel et al., 1995; Uceda et al., 1992; Wada et al., 1995). Little information is, however, available on the role of K_{Ca} channels in the presynaptic ACh release from splanchnic nerve endings.

We have recently developed a dialysis technique to simultaneously monitor the release of presynaptic ACh and postsynaptic catecholamine in the *in vivo* adrenal medulla (Akiyama et al., 2004a). This method makes it possible to investigate the functional roles of K_{Ca} channels in the ACh release from splanchnic nerve endings and the catecholamine release from adrenal medulla in the *in vivo* state. In the present study, we applied the microdialysis technique to the adrenal medulla of anesthetized rats and investigated the effects of K_{Ca} channel antagonists on the release of presynaptic ACh and postsynaptic catecholamine.

* Corresponding author. Tel.: +81 6 6833 5012x2380; fax: +81 6 6872 8092.
E-mail address: takiyama@ri.ncvc.go.jp (T. Akiyama).

0197-0186/$ – see front matter © 2009 Elsevier Ltd. All rights reserved.
doi:10.1016/j.neuint.2009.10.010

In electrophysiological studies, K_{Ca} channels can be divided into two types based on their single channel conductance: large-conductance (BK) and small-conductance K_{Ca} (SK) channels (Blatz and Magleby, 1987). We tested two types of BK channel antagonists: the selective peptidergic BK channel antagonist, iberiotoxin (Candia et al., 1992) and the non-peptidergic BK channel antagonist, paxilline (Kanus et al., 1994). Similarly we tested two types of SK channel antagonists: the selective peptidergic SK channel antagonist, apamin (Blatz and Magleby, 1986) and the selective peptidergic SK channel antagonist different in amino acid sequence, scyllatoxin (Auguste et al., 1990).

2. Materials and methods

2.1. Animal preparation

Animal care was provided in strict accordance with the *Guiding Principles for the Care and Use of Animals in the Field of Physiological Sciences* approved by the Physiological Society of Japan. All protocols were approved by the Animal Subject Committee of the National Cardiovascular Center. Adult male Wistar rats weighing 380–460 g were anesthetized with pentobarbital sodium (50–55 mg/kg, i.p.). A cervical midline incision was made to expose the trachea, which was then cannulated. The rats were ventilated with a constant-volume respirator using room air mixed with oxygen. The left femoral artery and vein were cannulated for monitoring arterial blood pressure and administration of anesthetic, respectively. The level of anesthesia was maintained with a continuous intravenous infusion of pentobarbital sodium (15–25 mg/kg/h, i.v.). The electrocardiogram was monitored to record the heart rate. A thermostatic heating pad was used to keep the esophageal temperature within a range of 37–38 °C. With the animal in the lateral position, the left adrenal gland and left splanchnic nerve were exposed by a subcostal flank incision, and the left splanchnic nerve was transected. In protocols requiring nerve stimulation, shielded bipolar stainless steel electrodes were applied to the distal end of the nerve, which was then stimulated with a digital stimulator (SEN-7203, Nihon Kohden, Japan) with a rectangular pulse (10 V and 1 ms in duration).

2.2. Dialysis technique

Dialysis probe construction was the same as that used in our previous dialysis experiments (Akiyama et al., 2003, 2004a,b). Each end of a dialysis fiber (0.32 mm OD, and 0.25 mm ID; PAN-DX 100,000 mol wt 100% cutoff, Asahi Chemical, Japan) was inserted into a polyethylene tube (25 cm length, 0.5 mm OD, and 0.2 mm ID; SP-8) and glued. The length of the dialysis fiber exposed was 3 mm. At a perfusion speed of 10 μl/min, *in vitro* recovery rates of ACh, norepinephrine (NE) and epinephrine (Epi) were (%): 3.21 ± 0.07, 2.68 ± 0.03, and 2.80 ± 0.03, respectively (number of dialysis probes: 3).

The left adrenal gland was gently lifted, and the dialysis probe was implanted in the medulla of the left adrenal gland along the long axis using a fine guiding needle. The dialysis probe was perfused with Ringer's solution or Ringer's solution containing pharmacological agents at a speed of 10 μl/min using a microinjection pump (CMA/100, Carnegie Medicin, Sweden). Ringer's solution consisted of (in mM) 147.0 NaCl, 4.0 KCl, 2.25 $CaCl_2$. All K_{Ca} channel antagonists tested were locally administered by perfusion through the dialysis probe after being dissolved in Ringer's solution. We started the protocols followed by a stabilization period of 3–4 h and sampled dialysate taking the dead space volume between the dialysis membrane and sample tube into account. Dialysate ACh and catecholamine concentrations were separately measured using each high-performance liquid chromatography with electrochemical detection as previously described (Akiyama et al., 2004a,b).

2.3. Experimental protocols

The experiment was performed based on the previous experiment showing that dialysate ACh and/or catecholamine responses were reproducible on repetition of the pharmacological or electrical stimulation (Akiyama et al., 2004a,b). At the end of the experiment, the rats were sacrificed with pentobarbital sodium, and the implant sites were examined. The dialysis probes were confirmed to have been implanted in the adrenal medulla, and no bleeding or necrosis was found macroscopically.

2.4. Protocol 1

We perfused the dialysis probe with Ringer's solution containing a cholinesterase inhibitor, neostigmine (10 μM) and investigated the effects of BK and SK channel antagonists on the nerve stimulation-induced responses of dialysate ACh and catecholamine concentration. The left splanchnic nerves were firstly electrically stimulated for 2 min at 2 Hz. Then, after a 30-min interval, nerves were subjected to a second stimulation for 2 min at 4 Hz. After these control stimulations, local administration of iberiotoxin (1 μM, $n = 7$), paxilline (100 μM, $n = 7$), apamin (10 μM, $n = 7$) or scyllatoxin (2 μM, $n = 7$) was started. Thirty minutes after local administration of K_{Ca} channel antagonists, nerves were stimulated for 2 min at 2 Hz. Next, after a 30-min interval, nerves were stimulated again for 2 min at 4 Hz. Phosphate buffer (pH 3.5, 4 μl) was transferred into each sample tube before dialysate sampling. Two dialysate samples were continuously collected per nerve stimulation: one before and one during stimulation. One sampling period was 2 min (1 sample volume = 20 μl). Half of the dialysate sample was used for the measurement of ACh, and the remaining half for the measurement of NE and Epi.

2.5. Protocol 2

We investigated the effects of K_{Ca} channel antagonists on the nerve stimulation-induced catecholamine release in the absence of neostigmine. Like in protocol 1, the left splanchnic nerves were stimulated before and 30 min after administration of iberiotoxin ($n = 7$), paxilline ($n = 7$), apamin ($n = 7$) or scyllatoxin ($n = 7$) and two dialysate samples were collected per nerve stimulation. The dialysate sample was used for the measurement of NE and Epi.

2.6. Protocol 3

We investigated the effects of K_{Ca} channel antagonists on exogenous ACh-induced catecholamine release. The dialysis probe was perfused with Ringer's solution. ACh (1 mM) was locally administered to the adrenal medulla through the dialysis probe for 1 min. After first administration of ACh, local administration of iberiotoxin (1 μM, $n = 7$), paxilline (100 μM, $n = 7$), apamin (10 μM, $n = 7$) or scyllatoxin (2 μM, $n = 7$) was started. Thirty minutes after local administration of K_{Ca} channel antagonists, ACh (1 mM) was locally administered again for 1 min. Phosphate buffer (pH 3.5, 2 μl) was transferred into each sample tube before dialysate sampling. Two dialysate samples were continuously collected per local administration of ACh: one before and one during administration. One sampling period was 1 min (1 sample volume = 10 μl). The dialysate sample was used for the measurement of NE and Epi.

2.7. Drugs

Drugs were mixed fresh for each experiment. Neostigmine methylsulfate (Shionogi, Japan), iberiotoxin (Peptide Institute, Japan), apamin (Peptide Institute) and scyllatoxin (Peptide Institute) were dissolved and diluted in Ringer's solution. Paxilline (Sigma Chemical, USA) was dissolved in DMSO and diluted in Ringer's solution. The final concentration of DMSO in the working solution was 0.5% (v/v).

2.8. Statistical methods

To examine the effects of nerve stimulation, local administration of ACh, and K_{Ca} channel antagonists, we analyzed heart rate and mean arterial pressure, basal dialysate NE and Epi content, and dialysate ACh, NE and Epi responses, by using one-way analysis of variance with repeated measures. When statistical significance was detected, the Newman–Keuls test was applied (Winer, 1971). Statistical significance was defined as $P < 0.05$. Values are presented as means ± SE.

3. Results

3.1. Changes in heart rate and mean arterial pressure

Local administration of neostigmine, K_{Ca} channel antagonists, and ACh through the dialysis probe did not change basal heart rate or mean arterial pressure. In protocol 1, nerve stimulation increased mean arterial pressure from 113 ± 3 mmHg in control to 131 ± 2 mmHg at 2 Hz ($n = 28$, $P < 0.05$) and 132 ± 2 mmHg at 4 Hz ($n = 28$, $P < 0.05$), and decreased heart rate from 436 ± 4 beats/min in control to 424 ± 4 beats/min at 2 Hz ($n = 28$, $P < 0.05$) and 420 ± 4 beats/min at 4 Hz ($n = 28$, $P < 0.05$). In protocol 2, nerve stimulation increased mean arterial pressure from 115 ± 4 mmHg in control to 129 ± 3 mmHg at 2 Hz ($n = 28$, $P < 0.05$) and 131 ± 3 mmHg at 4 Hz ($n = 28$, $P < 0.05$), and decreased heart rate from 423 ± 3 beats/min in control to 410 ± 4 beats/min at 2 Hz ($n = 28$, $P < 0.05$) and 404 ± 3 beats/min at 4 Hz ($n = 28$, $P < 0.05$). Heart rate and mean arterial pressure recovered to basal levels after nerve stimulation. After administration of K_{Ca} channel antagonists, nerve stimulation evoked the same responses of heart rate and mean arterial pressure.

Please cite this article in press as: Akiyama, T., et al., Role of Ca^{2+}-activated K^+ channels in catecholamine release from *in vivo* rat adrenal medulla. Neurochem. Int. (2009), doi:10.1016/j.neuint.2009.10.010

Table 1
Basal NE and Epi release before and after local administration of K_{Ca} channel antagonists.

	NE (nM)	Epi (nM)
Iberiotoxin ($n=21$)		
Before administration	4.8 ± 0.3	16.7 ± 1.0
After administration	5.0 ± 0.4	21.7 ± 1.6*
Paxilline ($n=21$)		
Before administration	4.7 ± 0.3	15.7 ± 1.1
After administration	4.8 ± 0.4	22.0 ± 1.9*
Apamin ($n=21$)		
Before administration	4.9 ± 0.4	17.1 ± 1.1
After administration	4.6 ± 0.5	21.2 ± 1.6*
Scyllatoxin ($n=21$)		
Before administration	4.9 ± 0.3	15.3 ± 0.7
After administration	5.1 ± 0.4	20.6 ± 0.9*

Values are means ± SE. n, no. of rats; NE, norepinephrine; Epi, epinephrine. *$P < 0.05$ vs. values before administration.

3.2. Basal ACh and catecholamine release

ACh could not be detected in dialysate before nerve stimulation even in the presence of neostigmine. In contrast, substantial amounts of NE and Epi were observed in dialysate before nerve stimulation or ACh administration. Local administration of neostigmine did not influence this basal catecholamine release. BK channel antagonists, iberiotoxin and paxilline did not change basal NE release but increased basal Epi release. Similarly, the SK channel antagonists, apamin and scyllatoxin did not change basal NE release, but increased basal Epi release (Table 1).

ACh was detected in dialysate only during nerve stimulation in the presence of neostigmine. Thus, we expressed this detected dialysate ACh concentration as an index of ACh release induced by nerve stimulation. In contrast, we subtracted basal dialysate NE and Epi content before nerve stimulation or ACh administration from those during stimulation or ACh administration, and expressed these subtracted values as indices of NE and Epi release induced by nerve stimulation or ACh administration.

3.3. Effects of K_{Ca} channel antagonists on the nerve stimulation-induced ACh and catecholamine release in the presence of neostigmine

Iberiotoxin enhanced the nerve stimulation-induced release of presynaptic ACh and postsynaptic catecholamine (Fig. 1A). ACh release increased from 4.5 ± 0.8 to 7.4 ± 0.7 nM at 2 Hz and from 9.4 ± 1.0 to 14.0 ± 1.0 nM at 4 Hz. NE release increased from 7 ± 0.5 to 32 ± 3 nM at 2 Hz and from 27 ± 3 to 74 ± 9 nM at 4 Hz. Epi release increased from 39 ± 5 to 78 ± 5 nM at 2 Hz, and from 105 ± 8 to 193 ± 15 nM at 4 Hz. Similarly, paxilline enhanced the nerve stimulation-induced release of ACh and catecholamine (Fig. 1B). ACh release increased from 4.1 ± 0.4 to 5.9 ± 0.5 nM at 2 Hz and from 9.4 ± 0.7 to 13.7 ± 0.9 nM at 4 Hz. NE release increased from 11 ± 2 to 26 ± 4 nM at 2 Hz, from 31 ± 5 to 58 ± 8 nM at 4 Hz. Epi release increased from 41 ± 7 to 77 ± 14 nM at 2 Hz and from 108 ± 14 to 195 ± 17 nM at 4 Hz.

Apamin had no effect on the nerve stimulation-induced release of ACh and NE, but enhanced the nerve stimulation-induced Epi release (Fig. 2A). Epi release increased from 45 ± 3 to 59 ± 4 nM at 2 Hz and from 108 ± 7 to 139 ± 17 nM at 4 Hz. Scyllatoxin had no effect on the nerve stimulation-induced release of ACh and NE either, but enhanced the nerve stimulation-induced Epi release (Fig. 2B). Epi release increased from 37 ± 4 to 50 ± 3 nM at 2 Hz and from 122 ± 5 to 152 ± 12 nM at 4 Hz.

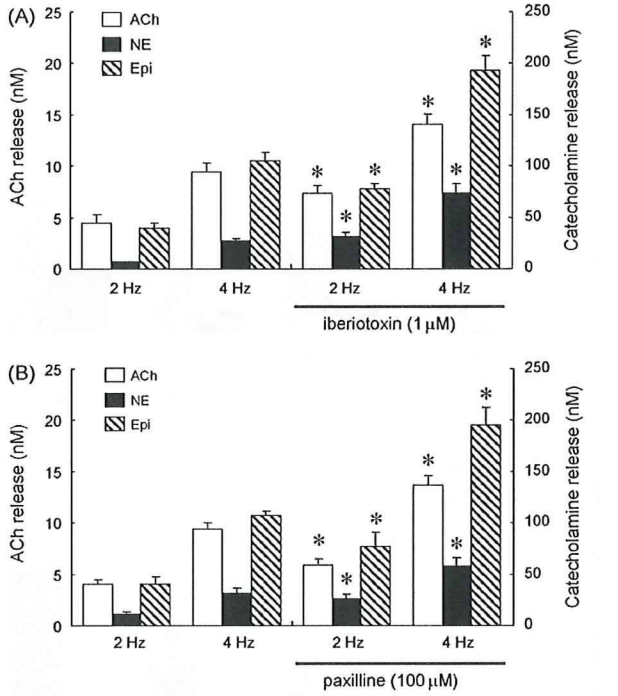

Fig. 1. Effects of BK channel antagonists on the nerve stimulation-induced release of acetylcholine (ACh), norepinephrine (NE) and epinephrine (Epi) in the presence of neostigmine (10 μM): iberiotoxin (A) and paxilline (B) enhanced the release of ACh, NE and Epi at 2 and 4 Hz. Values are means ± SE from seven rats. *$P < 0.05$ vs. ACh, NE or Epi release at the same frequency as before administration of BK channel antagonists.

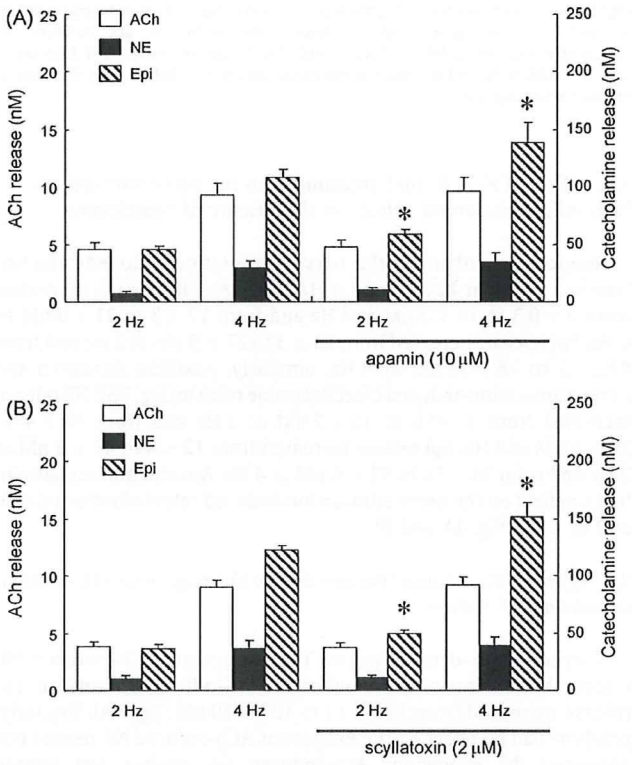

Fig. 2. Effects of SK channel antagonists on the nerve stimulation-induced release of ACh, NE and Epi in the presence of neostigmine (10 μM): apamin (A) and scyllatoxin (B) had no effect on the release of ACh or NE, but enhanced the Epi release at 2 and 4 Hz. Values are means ± SE from seven rats. *$P < 0.05$ vs. ACh, NE or Epi release at the same frequency as before administration of SK channel antagonists.

Please cite this article in press as: Akiyama, T., et al., Role of Ca^{2+}-activated K^+ channels in catecholamine release from *in vivo* rat adrenal medulla. Neurochem. Int. (2009), doi:10.1016/j.neuint.2009.10.010

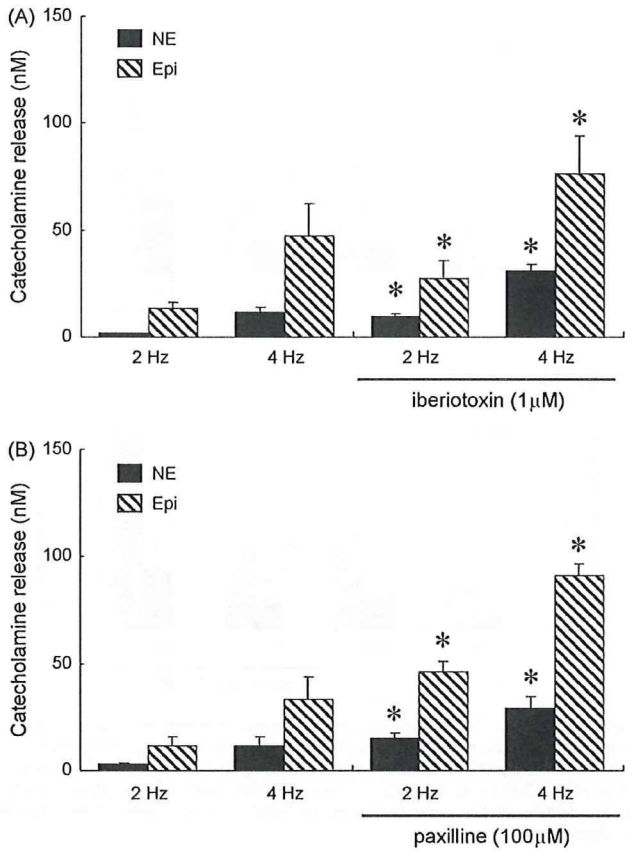

Fig. 3. Effects of BK channel antagonists on the nerve stimulation-induced release of NE and Epi in the absence of neostigmine: iberiotoxin (A) and paxilline (B) enhanced the release of NE and Epi at 2 and 4 Hz. Values are means ± SE from seven rats. *$P < 0.05$ vs. NE or Epi release at the same frequency as before administration of BK channel antagonists.

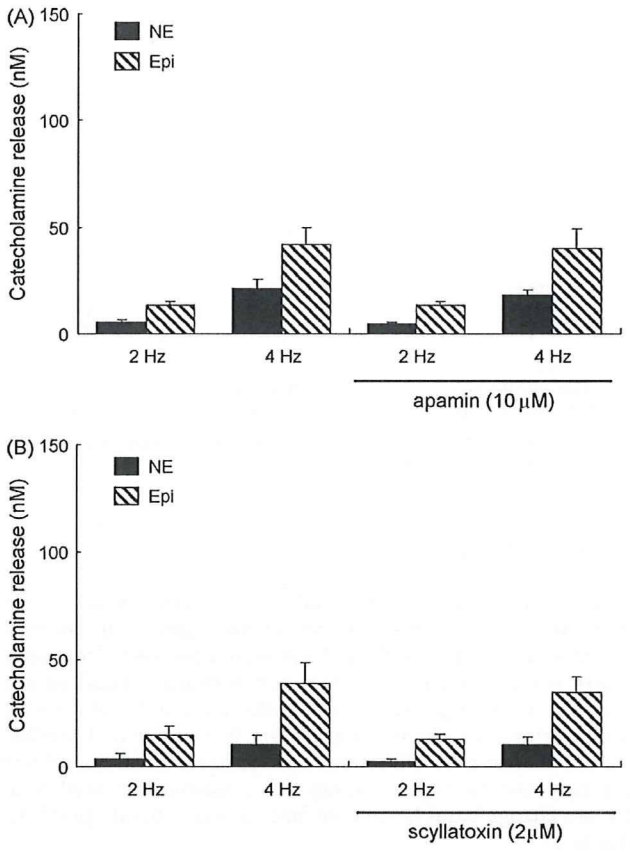

Fig. 4. Effects of SK channel antagonists on the nerve stimulation-induced release of NE and Epi in the absence of neostigmine: apamin (A) and scyllatoxin (B) had no effect on the release of NE or Epi at 2 or 4 Hz. Values are means ± SE from seven rats.

3.4. Effects of K_{Ca} channel antagonists on the nerve stimulation-induced catecholamine release in the absence of neostigmine

Iberiotoxin enhanced the nerve stimulation-induced catecholamine release at both 2 and 4 Hz (Fig. 3A). NE release increased from 2 ± 0.3 to 10 ± 2 nM at 2 Hz and from 12 ± 3 to 31 ± 3 nM at 4 Hz. Epi release increased from 13 ± 3 to 27 ± 9 nM at 2 Hz and from 47 ± 15 to 76 ± 18 nM at 4 Hz. Similarly, paxilline enhanced the nerve stimulation-induced catecholamine release (Fig. 3B). NE release increased from 3 ± 0.6 to 15 ± 2 nM at 2 Hz and from 12 ± 4 to 29 ± 5 nM at 4 Hz. Epi release increased from 12 ± 4 to 46 ± 5 nM at 2 Hz and from 34 ± 10 to 91 ± 6 nM at 4 Hz. Apamin and scyllatoxin had no effect on the nerve stimulation-induced catecholamine release at 2 or 4 Hz (Fig. 4A and B).

3.5. Effects of K_{Ca} channel antagonists on the exogenous ACh-induced catecholamine release

Iberiotoxin had no effect on the exogenous ACh-induced NE release, but enhanced the exogenous ACh-induced Epi release. Epi release increased from 108 ± 11 to 127 ± 10 nM (Fig. 5A). Similarly, paxilline had no effect on the exogenous ACh-induced NE release but enhanced the exogenous ACh-induced Epi release. Epi release increased from 93 ± 5 to 137 ± 13 nM (Fig. 5B). Apamin enhanced the exogenous ACh-induced catecholamine release (Fig. 6A). NE release increased from 37 ± 4 to 49 ± 4 nM and Epi release from 103 ± 8 to 122 ± 9 nM. Similarly scyllatoxin enhanced the exogenous ACh-induced catecholamine release (Fig. 6B). NE release increased from 32 ± 3 to 47 ± 3 nM and Epi release from 108 ± 6 to 140 ± 11 nM.

4. Discussion

4.1. Roles of K_{Ca} channels on splanchnic nerve endings in presynaptic ACh release

We found that, in the *in vivo* adrenal medulla, both iberiotoxin and paxilline enhanced the nerve stimulation-induced release of presynaptic ACh at 2 and 4 Hz by ~50% in the presence of neostigmine (Fig. 1). BK channels currents have been confirmed on cholinergic nerve endings including motor nerves in the neuromuscular junction (Flink and Atchison, 2003), presynaptic nerves in the chick ciliary ganglion (Sun et al., 1999) and tracheal parasympathetic nerves (Zhang et al., 1998). Activation of the K_{Ca} conductance is considered to limit Ca^{2+} entry through voltage-dependent Ca^{2+}channels, and subsequently reduce transmitter release (Meir et al., 1999). Our results strongly suggest that BK channels are present on the splanchnic nerve endings and involved in the control of ACh release. In the perfused cat adrenal gland, charybdotoxin, a BK channel antagonist, enhanced catecholamine release when transmural electrical stimulation was applied at low external Ca^{2+} concentrations, but not when exogenous ACh was administered (Montiel et al., 1995). In the perfused rat adrenal gland, charybdotoxin enhanced the release of Epi and NE induced by transmural electrical stimulation, but not the release induced by administration of ACh (Nagayama et al., 2000b). These indirect studies suggested that BK channels may be involved in the control

Please cite this article in press as: Akiyama, T., et al., Role of Ca^{2+}-activated K^+ channels in catecholamine release from *in vivo* rat adrenal medulla. Neurochem. Int. (2009), doi:10.1016/j.neuint.2009.10.010

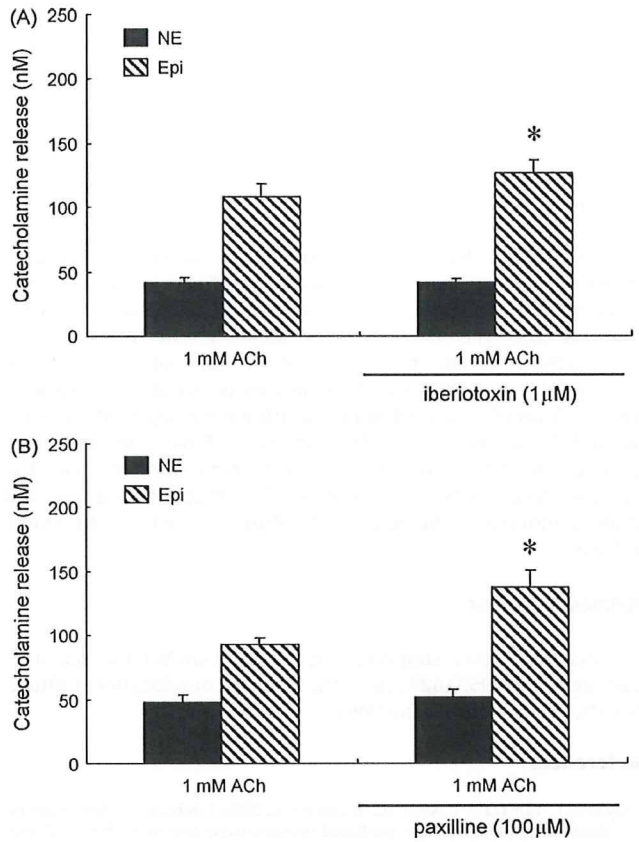

Fig. 5. Effects of BK channel antagonists on the exogenous ACh-induced release of NE and Epi: iberiotoxin (A) and paxilline (B) had no effect on NE release, but enhanced Epi release. Values are means ± SE from seven rats. *$P < 0.05$ vs. NE or Epi release before administration of BK channel antagonists.

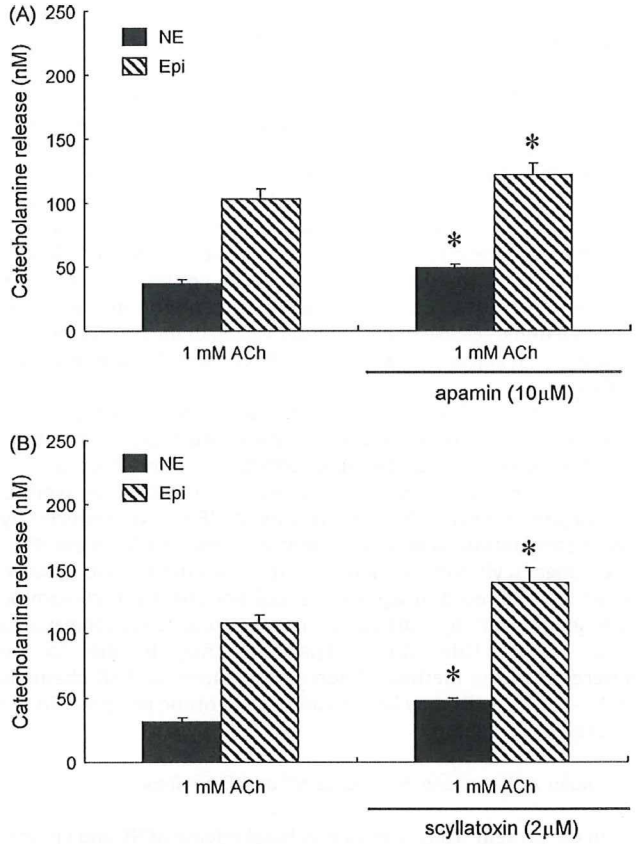

Fig. 6. Effects of SK channel antagonists on the exogenous ACh-induced release of NE and Epi: apamin (A) and scyllatoxin (B) enhanced the release of NE and Epi. Values are means ± SE from seven rats. *$P < 0.05$ vs. NE or Epi release before administration of SK channel antagonists.

of catecholamine release at the presynaptic site. But there has been no direct study investigating the effect of BK channel antagonists on ACh release from splanchnic nerve endings. This is the first direct study to demonstrate that BK channels are involved in the control of ACh release from splanchnic nerve endings. In the *in vivo* adrenal medulla, we observed a substantial enhancement of ACh release by BK channel antagonists at a frequency of 2 Hz with this degree of enhancement being similar to that at a frequency of 4 Hz (Fig. 1). BK channels on splanchnic nerve endings could be functional under physiological conditions. In our previous study, the nerve stimulation-induced catecholamine release was in large part cholinergic in the presence or absence of neostigmine (Akiyama et al., 2003). Thus, BK channels play an inhibitory role in the physiological catecholamine release from adrenal medulla by limiting presynaptic ACh release.

In contrast to BK channel antagonists, apamin and scyllatoxin had no effect on the nerve stimulation-induced ACh release at 2 or 4 Hz (Fig. 2). In perfused cat adrenal glands preloaded with [^{3}H]-choline, apamin did not modify the efflux of [^{3}H]-labeled compound evoked by transmural electrical stimulation (Montiel et al., 1995). SK channels seem to be absent on splanchnic nerve endings or play a minor role in the ACh release from splanchnic nerve endings.

4.2. Role of K_{Ca} channels on chromaffin cells in catecholamine release

Iberiotoxin and paxilline had no effect on the exogenous ACh-induced NE release, but enhanced exogenous ACh-induced Epi release (Fig. 5). Adrenal chromaffin cells are divided into two populations: NE- and Epi-storing cells (Coupland, 1984). While BK channels seem to be absent on NE-storing cells or play a minor role in the nerve stimulation-induced NE release, BK channels seem to be present on Epi-storing cells. It has been reported that BK channels present at rat chromaffin cells are activated by Ca^{2+} influx and contribute to the rapid termination of action potentials (Prakriya and Lingle, 1999), while iberiotoxin augments the nicotinic receptor-mediated catecholamine secretion from bovine adrenal chromaffin cells (Wada et al., 1995). The enhancement by BK channel antagonists of nerve stimulation-induced Epi release may be in part ascribed to their direct effects on Epi-storing cells. BK channels on Epi-storing cells may be involved in the control of nerve stimulation-induced Epi release. In perfused rat and cat adrenal glands, charybdotoxin, a BK channel antagonist, does not affect the exogenous ACh-induced catecholamine release (Montiel et al., 1995; Nagayama et al., 2000b). Our results of Epi release were inconsistent with these studies, possibly due to differences in the BK channel antagonists used and/or in methodology because charybdotoxin is pharmacologically less selective than iberiotoxin for BK channels (Garcia et al., 1991).

Both apamin and scyllatoxin enhanced the nerve stimulation-induced Epi release in the presence of neostigmine without changes in ACh release (Fig. 2), and the exogenous ACh-induced release of NE and Epi (Fig. 6). These results suggest that SK channels are present on both NE- and Epi-storing cells and that such enhancement is due to the direct effects of SK channel antagonists on chromaffin cells. Neither apamin nor scyllatoxin, however, had any effect on the nerve stimulation-induced NE release in the presence or absence of neostigmine, and the nerve

Please cite this article in press as: Akiyama, T., et al., Role of Ca^{2+}-activated K^+ channels in catecholamine release from *in vivo* rat adrenal medulla. Neurochem. Int. (2009), doi:10.1016/j.neuint.2009.10.010

stimulation-induced Epi release in the absence of neostigmine (Figs. 2 and 4). SK channels on chromaffin cells may play a minor role in the nerve stimulation-induced catecholamine release. It has been reported that SK channels on chromaffin cells are activated by muscarinic receptor stimulation (Nagayama et al., 2000a; Uceda et al., 1992). In our previous study of the same preparation, we demonstrated that muscarinic receptors are present on NE- and Epi-storing cells but play a minor role in the nerve stimulation-induced release of NE and Epi, and that cholinesterase inhibitor elicited muscarinic receptor-mediated Epi release when splanchnic nerve was stimulated (Akiyama et al., 2003). Therefore, SK channels on NE- and Epi-storing cells play an important role in the catecholamine release induced by activation of muscarinic or non-cholinergic receptors including PACAP receptor (Fukushima et al., 2002).

In the perfused rat adrenal gland, apamin enhanced NE release induced by transmural electrical stimulation and a nicotinic receptor agonist (Nagayama et al., 2000b). Therefore, SK channels on NE-storing cells could be activated by nicotinic as well as muscarinic receptors. But, our results of NE release induced by nerve stimulation were inconsistent with this study. In anesthetized dogs, scyllatoxin enhanced catecholamine release induced by a nicotinic receptor agonist but did not affect catecholamine release induced by splanchnic nerve stimulation (Nagayama et al., 1998). Thus, this inconsistency may be due to the difference in the method of nerve stimulation and SK channels on NE-storing cells may be activated by nicotinic receptors in the extrasynaptic region.

4.3. Roles of K_{Ca} channels in basal NE and Epi release

In the present study, substantial basal release of NE and Epi was observed in dialysate before nerve stimulation or ACh administration. Both BK and SK channel antagonists enhanced the basal Epi release but not the basal NE release. In our preparation, splanchnic nerves had been transected before control sampling and basal catecholamine release was not enhanced by a cholinesterase inhibitor, neostigmine. Furthermore, using the same preparation we demonstrated that basal catecholamine release is resistant to not only cholinergic antagonists, but also N-, P/Q-, and L-type Ca^{2+} channel antagonists (Akiyama et al., 2004b). Basal catecholamine release seems to be non-cholinergic and independent of Ca^{2+} influx through voltage-dependent Ca^{2+} channels. Ca^{2+} release from intracellular Ca^{2+} stores may be involved in this basal catecholamine release. It has been suggested in chromaffin cells that K_{Ca} channels on the cell surface are activated by Ca^{2+} release from intracellular Ca^{2+} stores (Ohta et al., 1998). On Epi-storing cells, BK and SK channels may play a role in the Epi release induced by Ca^{2+} release from intracellular Ca^{2+} stores.

4.4. Methodological considerations

Because previous results suggested that distribution across the dialysis membrane is required (Akiyama et al., 2003, 2004a), we used the K_{Ca} channel antagonists at a concentration 10 times higher than that required for complete channel blockade in experimental settings *in vitro*. Then, we tested two different types of selective BK and SK channel antagonists in the present study because higher concentrations of K_{Ca} channel antagonists might induce other pharmacological effects.

Cholinesterase inhibitor was necessary to monitor endogenous ACh even during the splanchnic nerve stimulation because released ACh is rapidly degraded by acetylcholinesterase before reaching the dialysis fiber. Then, we examined the effects of K_{Ca} channel antagonists in the presence or absence of neostigmine because neostigmine may influence the effects of K_{Ca} channel antagonists. Local administration of neostigmine enhanced the nerve stimulation-induced catecholamine release to about 2-fold before and after administration of K_{Ca} channel antagonists (Figs. 1 and 3). This enhancement could be due to the elevation of synaptic ACh levels by inhibition of acetylcholinesterase.

5. Conclusion

We applied dialysis technique to the adrenal medulla of anesthetized rats and investigated the effects of K_{Ca} channel antagonists on the presynaptic ACh release from splanchnic nerve endings and the postsynaptic catecholamine release from chromaffin cells. BK channels on presynaptic splanchnic nerve endings play an inhibitory role in the physiological catecholamine release from adrenal medulla by limiting presynaptic ACh release while SK channels do not. BK channels on Epi-storing cells may play an inhibitory role in the nerve stimulation-induced Epi release. SK channels are present on NE- and Epi-storing cells, but play a minor role in the nerve stimulation-induced catecholamine release.

Acknowledgment

This work was supported by a Grant-in-Aid for scientific research (No. 19591829) from the Ministry of Education, Culture, Sports, Science and Technology.

References

Akiyama, T., Yamazaki, T., Mori, H., Sunagawa, K., 2003. Inhibition of cholinesterase elicits muscarinic receptor-mediated synaptic transmission in the rat adrenal medulla. Auton. Neurosci. 107, 65–73.
Akiyama, T., Yamazaki, T., Mori, H., Sunagawa, K., 2004a. Simultaneous monitoring of acetylcholine and catecholamine release in the in vivo rat adrenal medulla. Neurochem. Int. 44, 497–503.
Akiyama, T., Yamazaki, T., Mori, H., Sunagawa, K., 2004b. Effects of Ca^{2+} channel antagonists on acetylcholine and catecholamine releases in the in vivo rat adrenal medulla. Am. J. Physiol. 287, R161–R166.
Auguste, P., Hugues, M., Gravé, B., Gesquière, J.C., Maes, P., Tartar, A., Romey, G., Schweitz, H., Lazdunski, M., 1990. Leiurotoxin I (scyllatoxin), a peptide ligand for Ca^{2+}-activated K^+ channels. J. Biol. Chem. 265, 4753–4759.
Blatz, A., Magleby, K.L., 1986. Single apamin-blocked Ca-activated K^+ channels of small conductance in cultured rat skeletal muscle. Nature 323, 718–720.
Blatz, A., Magleby, K.L., 1987. Calcium-activated potassium channels. Trends. Neurosci. 10, 463–467.
Candia, S., Garcia, M.L., Latorre, R., 1992. Mode of action of iberiotoxin, a potent blocker of the large conductance Ca^{2+}-activated K^+ channel. Biophys. J. 63, 583–590.
Coupland, R.E., 1965. The Natural History of the Chromaffin Cell. Longmans, London.
Coupland, R.E., 1984. Ultrastructural features of the mammalian adrenal medulla. In: Motta, P.M. (Ed.), Ultrastructure of Endocrine Cells and Tissues. Nijhoff, Boston, MA, pp. 168–179.
Flink, M.T., Atchison, W.D., 2003. Iberiotoxin-induced block of Ca^{2+}-activated K^+ channels induces dihydropyridine sensitivity of ACh release from mammalian motor nerve terminals. J. Pharmacol. Exp. Ther. 305, 646–652.
Fukushima, Y., Nagayama, T., Hikichi, H., Mizukami, K., Yoshida, M., Suzuki-Kusaba, M., Hisa, H., Kimura, T., Satoh, S., 2002. Role of K^+ channels in the PACAP-induced catecholamine secretion from the rat adrenal gland. Eur. J. Pharmacol. 437, 69–72.
García, A.G., García-De-Diego, A.M., Gandía, L., Borges, R., García-Sancho, J., 2006. Calcium signaling and exocytosis in adrenal chromaffin cells. Physiol. Rev. 86, 1093–1131.
Garcia, M.L., Galvez, A., Garcia-Calvo, M., King, V.F., Vazquez, J., Kaczorowski, G.J., 1991. Use of toxins to study potassium channels. J. Bioenerg. Biomembr. 23, 615–646.
Kanus, H.G., McManus, O.B., Lee, S.H., Schmalhofer, W.A., Galcia-Calvo, M., Helms, L.M., Sanchez, M., Giangiacomo, K., Reuben, J.P., Smith, A.B., 1994. Tremorgenic indole alkaloids potently inhibit smooth muscle high-conductance calcium-activated potassium channels. Biochemistry 33, 5819–5828.
Meir, A., Ginsburg, S., Butkevich, A., Kachalsky, S.G., Kaiserman, I., Ahdut, R., Demirgoren, S., Rahamimoff, R., 1999. Ion channels in presynaptic nerve terminals and control of transmitter release. Physiol. Rev. 79, 1019–1088.
Montiel, C., López, M.G., Sánchez-García, P., Maroto, R., Zapater, P., García, A.G., 1995. Contribution of SK and BK channels in the control of catecholamine release by electrical stimulation of the cat adrenal gland. J. Physiol. 486, 427–437.

Please cite this article in press as: Akiyama, T., et al., Role of Ca^{2+}-activated K^+ channels in catecholamine release from *in vivo* rat adrenal medulla. Neurochem. Int. (2009), doi:10.1016/j.neuint.2009.10.010

Nagayama, T., Fukushima, Y., Hikichi, H., Yoshida, M., Suzuki-Kusaba, M., Hisa, H., Kimura, T., Satoh, S., 2000a. Interaction of SK_{Ca} channels and L-type Ca^{2+} channels in catecholamine secretion in the rat adrenal gland. Am. J. Physiol. 279, R1731–R1736.

Nagayama, T., Fukushima, Y., Yoshida, M., Suzuki-Kusaba, M., Hisa, H., Kimura, T., Satoh, S., 2000b. Role of potassium channels in catecholamine secretion in the rat adrenal gland. Am. J. Physiol. 279, R448–R454.

Nagayama, T., Masada, K., Yoshida, M., Suzuki-Kusaba, M., Hisa, H., Kimura, T., Satoh, S., 1998. Role of K^+ channels in adrenal catecholamine secretion in anesthetized dogs. Am. J. Physiol. 274, R1125–R1130.

Ohta, T., Ito, S., Nakazato, Y., 1998. Ca^{2+}-dependent K^+ currents induced by muscarinic receptor activation in guinea pig adrenal chromaffin cells. J. Neurochem. 70, 1280–1288.

Prakriya, M., Lingle, C.J., 1999. BK channel activation by brief deporalizations requires Ca^{2+} influx through L- and Q-type Ca^{2+} channels in rat chromaffin cells. J. Neurophysiol. 81, 2267–2278.

Sun, X.P., Schlichter, L.C., Stanley, E.F., 1999. Single-channel properties of BK-type calcium-activated potassium channels at a cholinergic presynaptic nerve terminal. J. Physiol. 518, 639–651.

Uceda, G., Artalejo, A.R., López, M.G., Abad, F., Neher, E., García, A.G., 1992. Ca^{2+}-activated K^+ channels modulate muscarinic secretion in cat chromaffin cells. J. Physiol. 454, 213–230.

Wada, A., Urabe, M., Yuhi, T., Yamamoto, R., Yanagita, T., Niina, H., Kobayashi, H., 1995. Large- and small-conductance Ca^{2+}-activated K^+ channels: their role in the nicotinic receptor-mediated catecholamine secretion in bovine adrenal medulla. Naunyn Schmiedeberg's Arch. Pharmacol. 352, 545–549.

Winer, B.J., 1971. Statistical Principles in Experimental Design, 2nd ed. McGraw-Hill, New York.

Zhang, X.Y., Zhu, F.X., Robinson, N.E., 1998. Role of cAMP and neuronal K^+ channels on α_2-AR-induced inhibition of ACh release in equine trachea. Am. J. Physiol. 274, L827–L832.

Please cite this article in press as: Akiyama, T., et al., Role of Ca^{2+}-activated K^+ channels in catecholamine release from *in vivo* rat adrenal medulla. Neurochem. Int. (2009), doi:10.1016/j.neuint.2009.10.010

Circulation Journal
Official Journal of the Japanese Circulation Society
http://www.j-circ.or.jp

REVIEW

Oxidative Stress and Central Cardiovascular Regulation

– Pathogenesis of Hypertension and Therapeutic Aspects –

Yoshitaka Hirooka, MD; Yoji Sagara, MD; Takuya Kishi, MD; Kenji Sunagawa, MD

Oxidative stress is a key factor in the pathogenesis of hypertension and target organ damage, beginning in the earliest stages. Extensive evidence indicates that the pivotal role of oxidative stress in the pathogenesis of hypertension is due to its effects on the vasculature in relation to the development of atherosclerotic processes. It remains unclear, however, whether oxidative stress in the brain, particularly the autonomic nuclei (including the vasomotor center), has an important role in the occurrence and maintenance of hypertension via activation of the sympathetic nervous system. The aim of the present review is to describe the contribution of oxidative stress in the brain to the neural mechanisms that underlie hypertension, and discuss evidence that brain oxidative stress is a potential therapeutic target. (*Circ J* 2010; **74:** 827–835)

Key Words: Blood pressure; Brain; Heart rate; Hypertension; Sympathetic nervous system

Accumulating evidence indicates that the sympathetic nervous system plays an important role in the pathogenesis of hypertension.[1–3] Activation of the sympathetic nervous system is involved in the stages, clinical forms, 24-h blood pressure patterns, end-organ damage, and metabolic abnormalities of hypertension.[1–3] Although peripheral factors are also involved, the central nervous system (CNS) mechanisms are considered crucial.[3–7] The results of recent studies strongly suggest that central sympathetic outflow is increased in hypertension.[3–7] Increased oxidative stress is also involved in the pathogenesis of hypertension.[8] Although there have been many studies regarding target organ damage in hypertension, relatively few studies have addressed the role of oxidative stress in sympathetic nervous system activation.[9–11] Based on the role of angiotensin II (Ang II) in the generation of reactive oxygen species (ROS), the relationship between brain angiotensin and central sympathetic outflow has been examined.[12,13] Our group was the first to report that increased ROS generation in the brainstem contributes to the neural mechanisms of hypertension in hypertensive rats,[14] and we and other investigators have reported additional evidence to support this concept and the potential therapeutic aspects.[9–11] This review focuses on the role of oxidative stress within the brain in the neural pathogenesis of hypertension.

Increased Oxidative Stress in the Brain in Hypertension

Among the target organs of hypertensive vascular diseases, the brain is most affected by aging and oxidative stress.[15,16] Cell membranes in the brain contain a high concentration of polyunsaturated fatty acids. These fatty acids are targeted by ROS, which elicit chain reactions of lipid peroxidation. Oxidative stress is determined by measuring levels of thiobarbituric acid-reactive substances (TBARS), end products of lipid peroxidation. The levels of TBARS reflect those of malondialedehyde, although the assay is not specific for malondialedehyde.[15,17] There are some important points, however, for assessing the levels of TBARS.[17] The medium used for tissue preparation needs to contain a chelating agent and an antioxidant, and conditions for the assay must be kept constant. Therefore, we used another method for assessing the ROS production, which is electron spin resonance (ESR) spectroscopy. The amount of ROS was quantified by monitoring the time-dependent decay of the amplitude of the ESR spectra produced by the nitroxide radical 4-hydroxy-2,2,6,6-tetramethyl-piperidine-*N*-oxyl (hydroxyl-TEMPO) as a spin probe.[9,14] The signal decay of ESR spectroscopy reflects oxidative stress more directly. Also, it has an advantage for in vivo study.[18] We evaluated oxidative stress in the brains of stroke-prone spontaneously hypertensive rats (SHRSP) compared with normotensive Wistar–Kyoto (WKY) rats.[9,14] The rostral ventrolateral medulla (RVLM) is the major vasomotor center that determines basal sympathetic nervous system activity and it is essential for the maintenance of basal vasomotor tone.[3–7] Spontaneously hypertensive rats (SHR) or SHRSP exhibit increased sympathetic nervous system activity during the development of hypertension and are commonly used in experimental studies as models of human essential hypertension.[3–7] We previously investigated whether ROS are increased in the RVLM of SHRSP.[14] First, we found that ROS levels measured by TBARS and ESR spectroscopy were increased in the RVLM of SHRSP compared with WKY

Received February 19, 2010; revised manuscript received March 25, 2010; accepted March 26, 2010; released online April 15, 2010
Department of Cardiovascular Medicine, Kyushu University Graduate School of Medical Sciences, Fukuoka, Japan
Mailing address: Yoshitaka Hirooka, MD, Department of Cardiovascular Medicine, Kyushu University Graduate School of Medical Sciences, 3-1-1 Maidashi, Higashi-ku, Fukuoka 812-8582, Japan. E-mail: hyoshi@cardiol.med.kyushu-u.ac.jp
ISSN-1346-9843 doi:10.1253/circj.CJ-10-0153

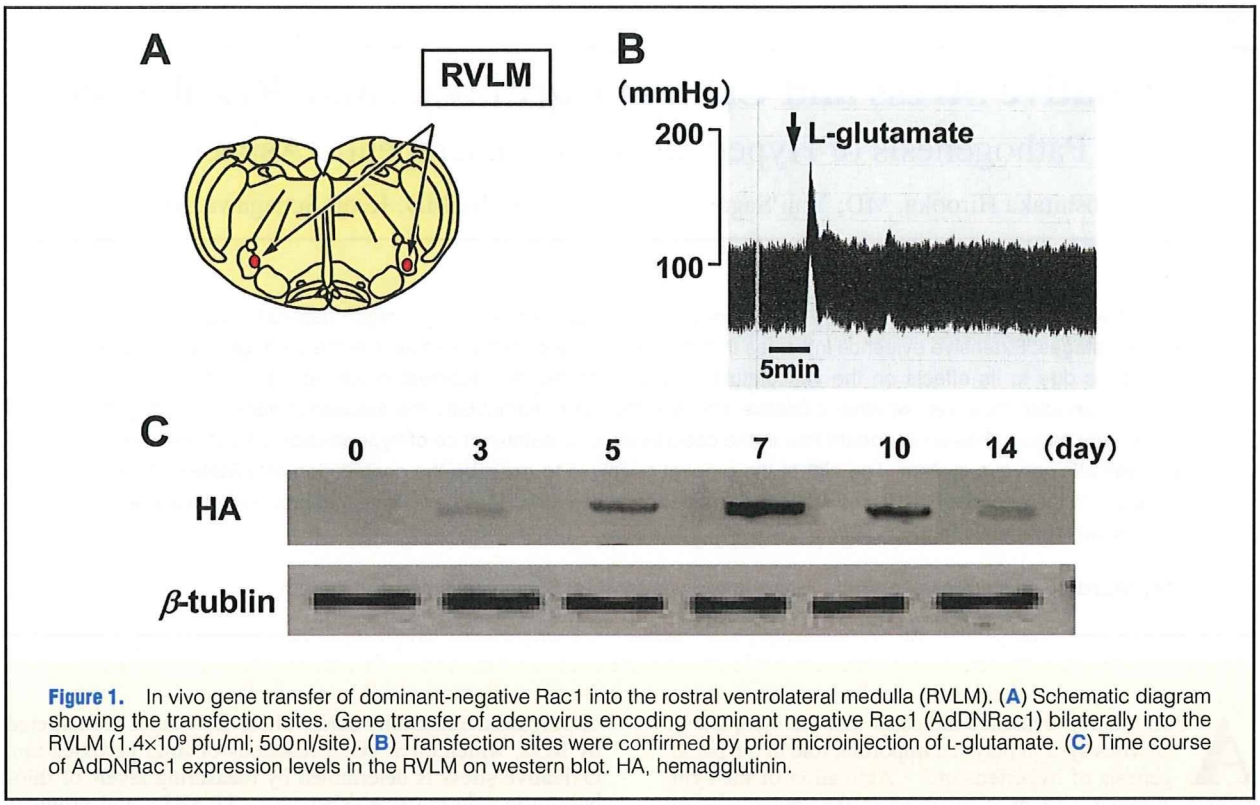

Figure 1. In vivo gene transfer of dominant-negative Rac1 into the rostral ventrolateral medulla (RVLM). (**A**) Schematic diagram showing the transfection sites. Gene transfer of adenovirus encoding dominant negative Rac1 (AdDNRac1) bilaterally into the RVLM (1.4×10^9 pfu/ml; 500 nl/site). (**B**) Transfection sites were confirmed by prior microinjection of L-glutamate. (**C**) Time course of AdDNRac1 expression levels in the RVLM on western blot. HA, hemagglutinin.

rats. In addition, superoxide dismutase (SOD) expression and activity, which are ROS scavenging factors, were decreased in the RVLM of SHRSP compared with WKY rats. Functionally, microinjection of the membrane-permeable radical scavenger tempol into the RVLM decreased blood pressure, heart rate, and sympathetic nervous system activity in SHRSP but not in WKY rats. More importantly, overexpression of Mn-SOD, an antioxidant enzyme, in the RVLM of SHRSP decreased blood pressure and sympathetic nervous system activity. These findings strongly indicate that oxidative stress in the RVLM is increased in SHRSP and contributes to the neural mechanisms of hypertension. As described here, brain ROS is one of the results of generalized target organ damage, appearing earlier in the brain due to its susceptibility. The brain ROS would increase blood pressure via activation of the sympathetic nervous system and this would ultimately result in a vicious cycle. It would be possible, however, that brain ROS is involved in the early stage of hypertension in SHR or SHRSP, because we found that oxidative stress in the brain assessed on in vivo ESR was enhanced in young (6-week-old) SHR or SHRSP compared with age-matched WKY rats (unpublished data). The levels of TBARS were not different, probably because the levels of TBARS reflect lipid peroxidation caused by ROS. Other investigators also found that an increase in superoxide anions in the RVLM is associated with hypertension in SHR,[19] and reduced expression and activity in Cu/Zn-SOD and Mn-SOD within the RVLM contribute to oxidative stress and neurogenic hypertension in SHR.[20] An increase in oxidative stress within the RVLM also plays an important role in maintaining high arterial blood pressure and sympathetic activation in 2-kidney 1-clip (2K-1C) hypertensive rats, which is a renovascular hypertension model.[21] In that study, Oliveira-Sales et al demonstrated that the mRNA expression of NAD(P)H oxidase subunits ($p47^{phox}$ and $gp91^{phox}$) in the RVLM was greater in 2K-1C than in the control group. Interestingly, there were no differences in Cu/Zn-SOD expression between the two groups. TBARS levels in the RVLM were significantly greater in the 2K-1C than in the control group, suggesting enhanced oxidative stress. Functionally, microinjection of vitamin C into the RVLM decreased blood pressure and renal sympathetic nerve activity in 2K-1C but not in controls. Importantly, in a subsequent study, these authors suggested that the paraventricular nucleus of the hypothalamus is also involved.[22] Notably, although 2K-1C is a model of renovascular hypertension, suggesting that circulating Ang II is increased, angiotensin type I (AT1) receptor gene expression levels within the RVLM and paraventricular nucleus were upregulated in this model, indicating that ROS was produced via the activation of nicotinamide-adenine dinucleotide phosphate [NAD(P)H] oxidase.

Sources of ROS Production in the Brain

As a source of ROS production in the CNS, NAD(P)H oxidase is a major player. NAD(P)H oxidase is composed of two membrane-bound subunits, $gp91^{phox}$ and $p22^{phox}$; several cytoplasmic subunits, $p47^{phox}$, $p40^{phox}$, and $p67^{phox}$; and the small G-protein Rac1.[23–26] Stimulation of AT1 receptors activates NAD(P)H oxidase by which the cytoplasmic subunits of Rac1NAD(P)H oxidase such as Rac1 bind to the membrane subunits, thereby activating the enzyme leading to superoxide generation. Rac1 requires lipid modification to migrate from the cytosol to the plasma membrane, which is a necessary step for activating ROS-generating NAD(P)H oxidase. NAD(P)H oxidase activity is greater in the brainstem of SHRSP than in that of WKY.[27,28] We transfected adenovirus

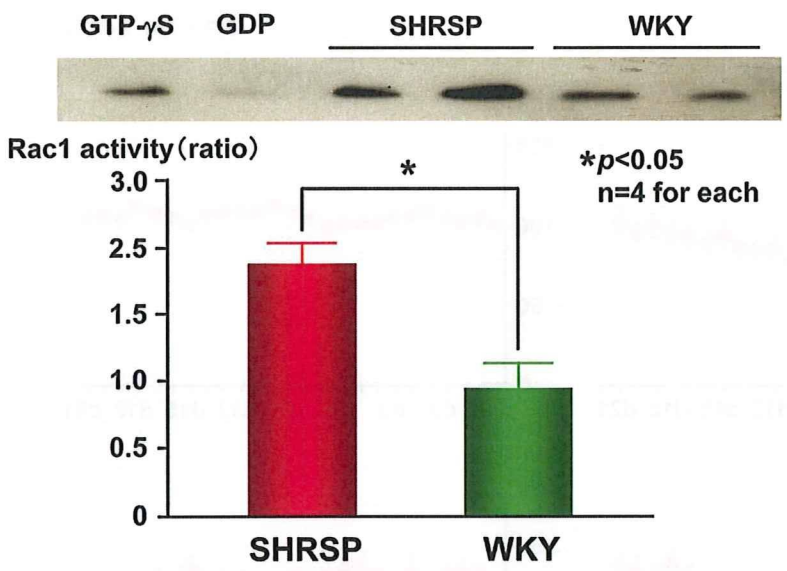

Figure 2. Rac1 activity is elevated in the rostral ventrolateral medulla of stroke-prone spontaneously hypertensive rats (SHRSP) compared to Wistar–Kyoto (WKY) rats. GDP, guanosine 5'-diphosphate; GTP-γS, guanosine 5'-*O*-(3-thiotriphospahte).

encoding dominant-negative Rac1 into the RVLM of SHRSP and WKY rats (Figure 1).[27] Rac1 activity in the RVLM tissue was increased in SHRSP compared to WKY rats (Figure 2).[27] Importantly, we demonstrated that inhibition of Rac1-derived ROS in the RVLM decreased blood pressure, heart rate, and urinary norepinephrine excretion in SHRSP (Figure 3).[27] A similar response occurs after inhibition of Rac1-derived ROS in the nucleus tractus solitarius (NTS).[28]

In addition to the cytosolic production of ROS, mitochondria are the primary source of ROS production in many cells. Ang II increases mitochondrial ROS production in the RVLM, leading to sympathoexcitation.[29] Furthermore, NAD(P)H oxidase-derived ROS might trigger Ca^{2+} accumulation, which leads to mitochondrial ROS production.[29] This suggestion is based on the finding that gene transfer of dominant negative Rac1 attenuated the Ang II-induced increase in reduced Mito-Tracker red fluorescence.[29] In contrast, impairment of mitochondrial electron transport chain complexes in the RVLM might be involved in the neural abnormality underlying hypertension in SHR.[30] This issue was recently discussed by Zimmerman and Zucker.[31] Although we did not detect impairment of brain mitochondrial respiratory complexes in SHRSP, we propose that mitochondria-derived ROS mediate sympathoexcitation via NAD(P)H oxidase activation.[29]

Another possibility for ROS generation is uncoupling nitric oxide synthase (NOS). In the absence of L-arginine or with tetrahydrobiopterin, NO production from inducible NOS (iNOS) causes uncoupling from the oxidation of NADPH, resulting in superoxide generation.[9] iNOS overexpression in the RVLM causes hypertension and sympathoexcitation that is mediated by an increase in oxidative stress.[32] This might be relevant to our observation that iNOS expression levels in the RVLM are greater in SHRSP than in WKY rats.[33] In addition, microinjection of iNOS antagonists into the RVLM reduces blood pressure only in SHR, but not in WKY rats.[33]

ROS-Mediated Activation of Transcriptional Factors

It has been suggested that an Ang II-mediated influx of Ca^{2+} in neurons depends on increased superoxide generation by a Rac1-dependent NAD(P)H oxidase.[34] Ang II also regulates neuronal activity via inhibition of the delayed rectifier potassium current.[35] Ang II-mediated upregulation of L-type Ca^{2+} currents in neurons isolated from the NTS is inhibited by scavenging ROS, indicating a role for NAD(P)H oxidase-derived superoxide in the activation of Ca^{2+} channels in the NTS.[24]

NAD(P)H oxidase-derived superoxide mediates an Ang II-induced pressor effect via the activation of p38 mitogen-activated protein kinase (MAPK) in the RVLM.[36] Recently, we suggested that AT1 receptor-activated caspase-3 acting through the Ras/p38 MAPK/extracellular signal-related protein kinase pathway in the RVLM is involved in sympathoexcitation in SHRSP.[37] These pathways may be downstream effectors of ROS in the RVLM, which in turn plays a crucial role in the pathogenesis of hypertension. Interestingly, the pro-apoptotic proteins Bax and Bad were enhanced and the anti-apoptotic protein Bcl-2 was decreased in the RVLM of SHRSP, and inhibition of caspase-3 normalized these changes in pro- and anti-apoptotic protein levels.[37] These alterations in the RVLM of SHRSP were stimulated by Ang II via activation of the AT1 receptors, which are upregulated in this strain and other hypertensive models.[38] It would be reasonable to consider that different mechanisms may be responsible for sympathoexcitation in different brain sites (influx of Ca^{2+} for RVLM, apoptosis for NTS), and activation of the apoptotic pathway is involved in sympathoexcitation in the RVLM.[37] The exact physiologic implication of these observations requires further evaluation.

Effects of Angiotensin Receptor Blockers on Brain Oxidative Stress

The existence of an independent renin–angiotensin system in the brain is well established. Activation of the brain renin–angiotensin system substantially contributes to the development and maintenance of hypertension through activation of the sympathetic nervous system, vasopressin release, and drinking behavior.[39,40] There is considerable evidence that

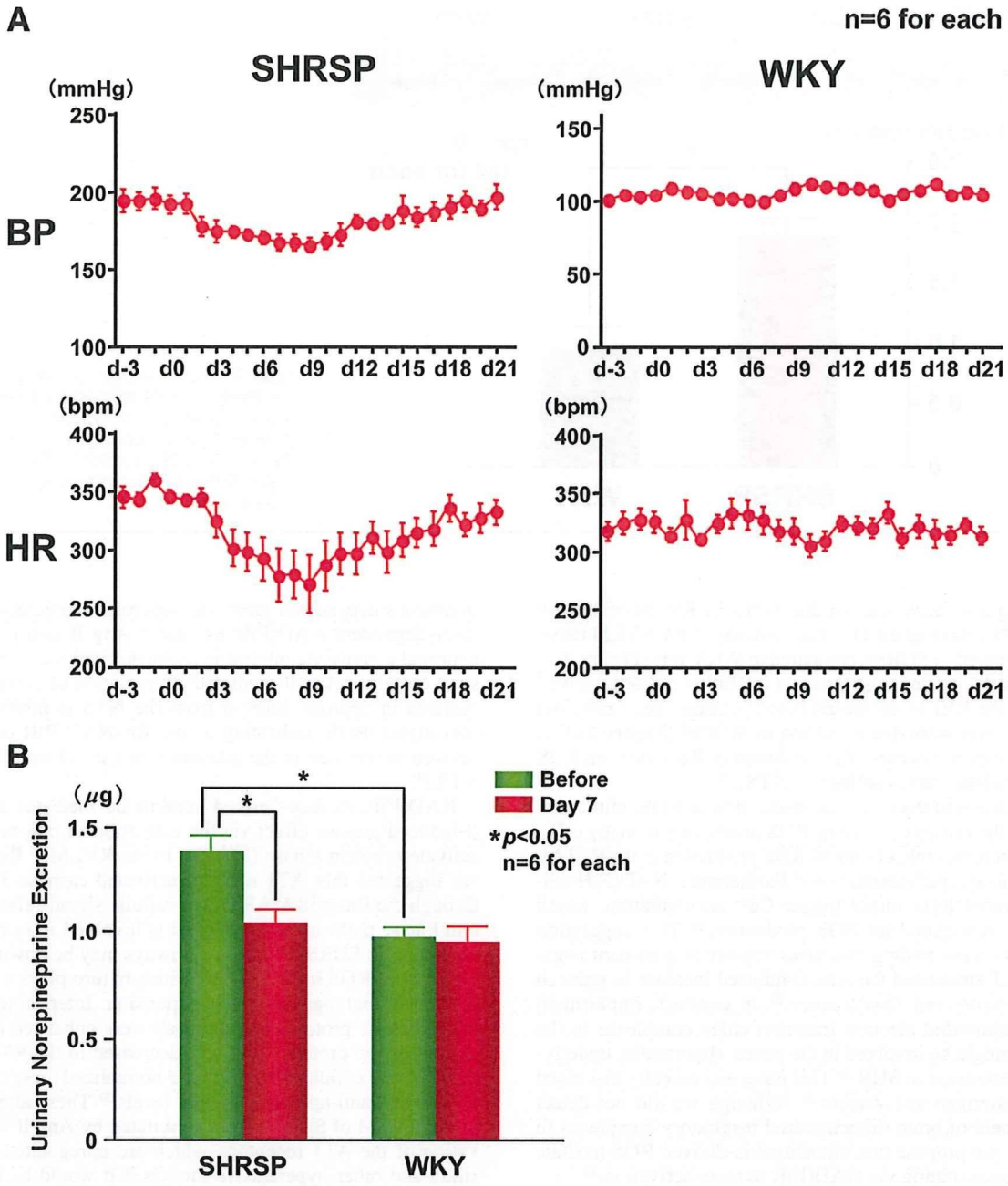

Figure 3. Inhibition of Rac1-dependent superoxide production in the rostral ventrolateral medulla (RVLM) decreases blood pressure, heart rate, and urinary norepinephrine excretion in stroke-prone spontaneously hypertensive rats (SHRSP). (A) Time course of mean blood pressure (BP) and heart rate (HR) before and after gene transfer of dominant negative Rac1 (DNRac1). (B) Twenty-four-hour urinary norepinephrine excretion before and after gene transfer of DNRac1 into the RVLM. d, day; WKY, Wistar–Kyoto rats.

peripherally administered angiotensin receptor blockers (ARBs) penetrate the blood–brain barrier, although there are some differences among ARBs.[41,42] AT1 receptors are abundant in the circumventricular organs, such as the subfornical organ and the organum vasculosum lamina terminalis, and the area postrema, which lack a blood–brain barrier.[39–42] Therefore, peripherally administered ARBs can also bind to those areas, thereby inhibiting the central actions of Ang II. Oral treatment with the ARB telmisartan appears to inhibit the central responses to Ang II in awake rats.[43] Although other ARBs also inhibit the central actions of Ang II within the brain beyond the blood–brain barrier,[41,42,44] these effects might differ depending on the pharmacokinetics and properties of each drug (ie, lipophilicity etc).[43] We evaluated the

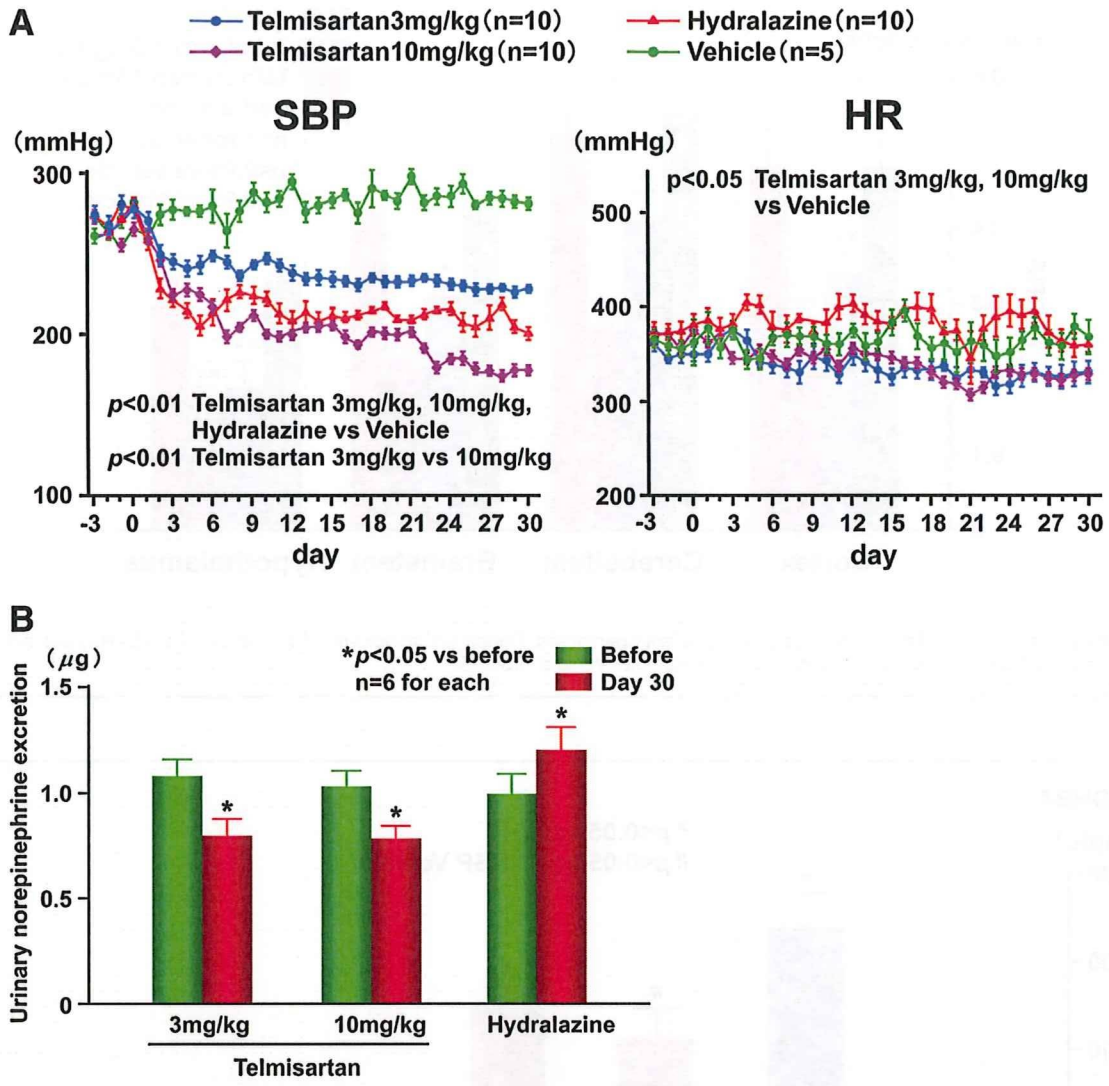

Figure 4. (A) Time course of changes in systolic blood pressure (SBP) and heart rate (HR) in SHRSP treated with telmisartan. (B) Telmisartan decreases 24-h urinary norepinephrine excretion at day 30, and hydralazine increases 24-h urinary norepinephrine excretion.

effect of treatment with telmisartan at either a high dose ($10\,mg \cdot kg^{-1} \cdot day^{-1}$) or a low dose ($3\,mg \cdot kg^{-1} \cdot day^{-1}$), or hydralazine for 30 days on hypertension.[45] Systolic blood pressure (SBP) and heart rate were measured using the tail-cuff method. Urinary norepinephrine excretion was measured as a marker of the sympathetic nervous system activity. We evaluated ROS in the brain (cortex, cerebellum, hypothalamus, and brainstem) of SHRSP on ESR spectroscopy and TBARS. Oral treatment with telmisartan reduced SBP dose-dependently and hydralazine reduced SBP to a similar level to the high dose of telmisartan (Figure 4). Telmisartan reduced, while hydralazine increased, urinary norepinephrine excretion (Figure 4). TBARS levels were significantly increased in each area of the brain of SHRSP compared with WKY rats (Figure 5). Oral treatment with telmisartan reduced the TBARS levels, but hydralazine did not (Figure 5). These findings suggest that (1) anti-hypertensive treatment with telmisartan reduces ROS in the brain of SHRSP; (2) telmisartan decreases blood pressure, at least in part, via a reduction of the sympathetic nervous system activity in SHRSP; and (3) these effects induced by telmisartan might be associated with protection of the brain of SHRSP from oxidative stress. We also measured the concentration of hydroxyl radicals using a modified procedure based on the hydroxylation of sodium salicylate by hydroxyl radicals,[46] leading to the production of 2,3-dihydroxybenzoic acid (2,3-DHBA).[29,47] Inhibition of Rac1 in the RVLM and oral treatment with telmisartan significantly decreased the production of hydroxyl radicals in the RVLM (Figure 6).[47]

Recently, we used in vivo ESR to assess oxidative stress in the brain, and found that oral treatment with another ARB, olmesartan, reduces oxidative stress in the brain of SHRSP without inducing reflex activation of the sympathetic nervous system.[48] In that study we evaluated the in vivo ESR signal

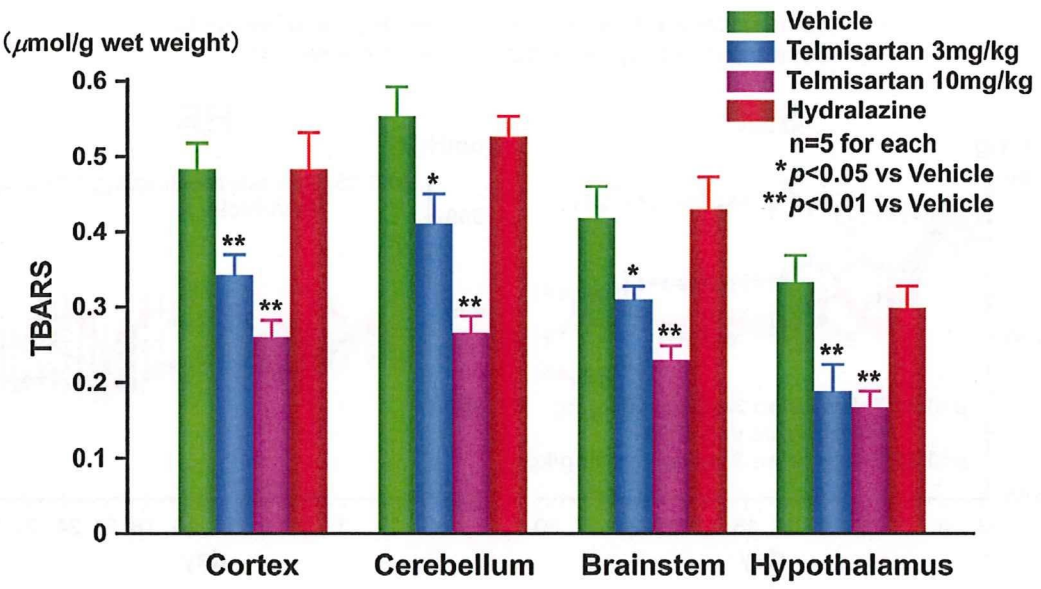

Figure 5. Antioxidant effects of telmisartan in different brain areas. Thiobarbituric acid-reactive substances (TBARS) levels after treatment with telmisartan (3 or 10mg/kg), hydralazine, or vehicle in SHRSP.

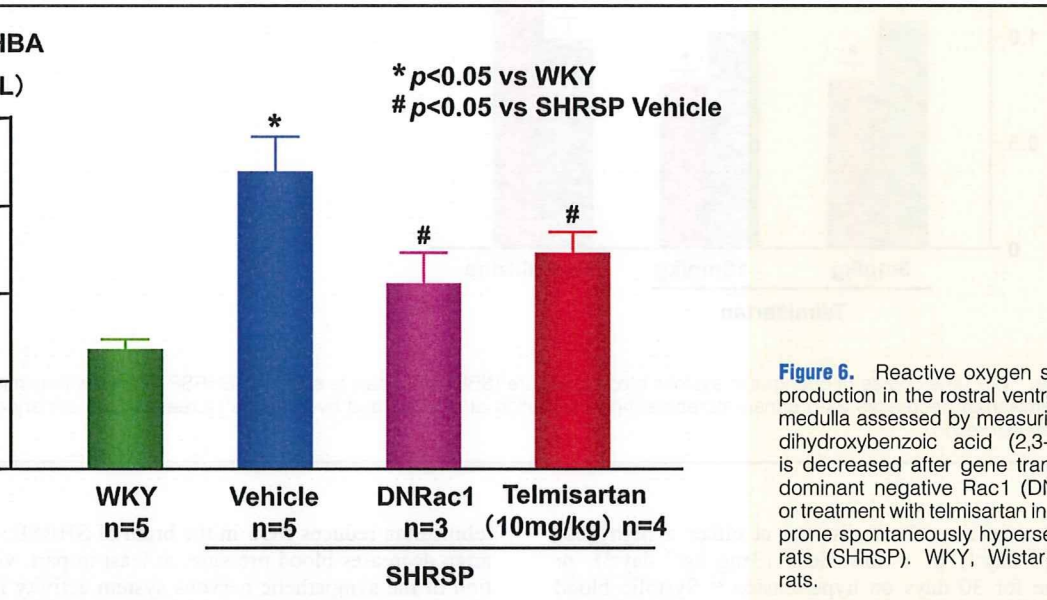

Figure 6. Reactive oxygen species production in the rostral ventrolateral medulla assessed by measuring 2,3-dihydroxybenzoic acid (2,3-DHBA) is decreased after gene transfer of dominant negative Rac1 (DNRac1) or treatment with telmisartan in stroke-prone spontaneously hypersensitive rats (SHRSP). WKY, Wistar–Kyoto rats.

decay rates of the brain using methoxycarbonyl-PROXYL, a nitroxyl radical species, as a blood–brain barrier-permeable spin probe.[49] Oral treatment with olmesartan attenuated the exaggerated pressor response to an excitatory amino acid, L-glutamate, in the RVLM of SHR compared to WKY rats.[50] Further, the pressor response to microinjection of Ang II into the RVLM was diminished in SHR treated with olmesartan.[50] Thus, the importance of oxidative stress in the brain and hypertension is supported by our studies as well as those of others.[11]

Several questions, however, remain to be answered. A recent study suggested that systemic administration of candesartan reduces brain Ang II levels because it attenuates the mRNA expression of both angiotensinogen and angiotensin-converting enzyme in Ang II-infused rats.[51] Whether systemic treatment with ARBs indirectly regulates brain Ang II remains to be determined.[52]

Effects of Other Cardiovascular Drugs on Brain Oxidative Stress

Considering that ARBs act to inhibit NAD(P)H oxidase activ-

ity, it is reasonable that ARBs have an antioxidant effect, although there are some unresolved questions, as mentioned previously. Calcium channel blockers, azelnidipine and amlodipine, but not nicardipine, which also have antioxidant properties, have a sympatho-inhibitory effect on the brain.[53,54] In particular, treatment with azelnidipine reduces oxidative stress in the RVLM associated with a decrease in the activity of NAD(P)H oxidase, Cu/Zn-SOD, and Mn-SOD.[53] These effects might be related to an improvement in NO production,[55] because we also demonstrated that overexpression of endothelial NOS in the NTS or RVLM decreases blood pressure and heart rate via the inhibition of sympathetic nervous system activity.[56–59] Surprisingly, we also found that atorvastatin inhibits the sympathetic nervous system as a result of upregulating NO activity and reducing oxidative stress.[60–63] Further studies are needed to determine if this mechanism is also applicable in humans.

Salt-Sensitive Hypertension and Brain Oxidative Stress

Activation of the sympathetic nervous system, in particular, an increase in central sympathetic outflow, plays an important role in the pathogenesis of salt-sensitive hypertension as well as that of kidney diseases.[64,65] Recent studies suggest that oxidative stress in the brain contributes to blood pressure elevation in salt-sensitive hypertension.[66,67] We demonstrated that high salt intake exacerbates blood pressure elevation and sympathetic nervous system activity during the development of hypertension in SHR, and these responses are mediated by increased ROS generation, probably because of an upregulation of AT1 receptors and NAD(P)H oxidase in the RVLM.[66] The findings of a recent study from Kyushu University Graduate School of Medical Sciences indicate that mice with pressure overload acquired brain salt-sensitivity.[68] This means that high salt intake increases the transport from the blood to the cerebrospinal fluid and the response of the sympathetic nerve activity to salt administered into the brain. These results suggest that pressure overload affects salt sensitivity, thereby enhancing central sympathetic outflow and cardiac function.[68] Left ventricular hypertrophy is an independent risk of cardiovascular event and high salt intake is an important environmental factor of hypertension, both of which increased ROS, and sympathoexcitation may be involved in the pathogenesis of the development of hypertension. A recent clinical trial suggested that left ventricular hypertrophy is related to cardiovascular events in Japanese high-risk hypertensive patients.[69]

Summary and Future Perspectives

Currently in Japan, many patients with hypertension also have metabolic syndrome. Importantly, the prevalence of metabolic syndrome increases linearly with an increase in heart rate among Japanese men and women,[70] suggesting that activation of the sympathetic nervous system is involved in the pathogenesis of hypertension.[71] The prevalence of obstructive sleep apnea has increased as a result of the increase in the number of obese patients with hypertension. Obese patients with sleep apnea have enhanced central sympathetic outflow, which worsens hypertension and leads to cardiovascular events.[72] Further, there is considerable evidence that psychological stress is a major risk factor for cardiovascular diseases and events associated with hypertension.[73] Another therapeutic target for the treatment of hypertension is heart failure with a preserved ejection fraction.[74] As suggested here, salt-sensitivity might also be enhanced in these patients, thereby further enhancing central sympathetic outflow.[68] Oxidative stress in the brain as well as other organs might underlie these mechanisms. Future studies of the effects of oxidative stress in the brain are warranted and will provide useful information for the treatment of hypertension.

Acknowledgments

We thank the many collaborators at Kyushu University Graduate School of Medical Sciences for their help and advice. We also thank Professor emeritus Akira Takeshita (deceased last March) for his continuing encouragement and support of this series of studies. This series of studies was supported by Grants-in-Aid for Scientific Research from Japan Society for the Promotion of Science.

References

1. Grassi G. Assessment of sympathetic cardiovascular drive in human hypertension: Achievements and perspectives. *Hypertension* 2009; **54:** 690–697.
2. Esler M. Pathophysiology of the human sympathetic nervous system in cardiovascular diseases: The transition from mechanisms to medical management. *J Appl Physiol* 2010; **108:** 227–237.
3. Guyenet PG. The sympathetic control of blood pressure. *Nat Rev Neurosci* 2006; **7:** 335–346.
4. Dampney RAL. Functional organization of central pathways regulating the cardiovascular system. *Physiol Rev* 1994; **74:** 323–364.
5. Pilowsky PM, Goodchild AK. Baroreceptor reflex pathways and neurotransmitters: 10 years on. *J Hypertens* 2002; **20:** 1675–1688.
6. Sved AF, Ito S, Sved JC. Brainstem mechanisms of hypertension: Role of the rostral ventrolateral medulla. *Curr Hypertens Rep* 2003; **5:** 262–268.
7. Campos RR, Bergamaschi CT. Neurotransmission alterations in central cardiovascular control in experimental hypertension. *Curr Hypertens Rev* 2006; **2:** 193–198.
8. Paravicini T, Touyz RM. Redox signaling in hypertension. *Cardiovasc Res* 2006; **71:** 247–258.
9. Hirooka Y. Role of reactive oxygen species in brainstem in neural mechanisms of hypertension. *Auton Neurosci* 2008; **142:** 20–24.
10. Peterson JR, Sharma RV, Davisson RL. Reactive oxygen species in the neuropathogenesis of hypertension. *Curr Hypertens Rep* 2006; **8:** 232–241.
11. Campos RR. Oxidative stress in the brain and arterial hypertension. *Hypertens Res* 2009; **32:** 1047–1048.
12. Zimmerman MC, Lazartigues E, Lang JA, Sinnayah P, Ahmad IM, Spitz DR, et al. Superoxide mediates the action of angiotensin II in the central nervous system. *Circ Res* 2002; **91:** 1038–1045.
13. Zimmerman MC, Lazartigues E, Sharma RV, Davisson RL. Hypertension caused by angiotensin II infusion involves increased superoxide production in the central nervous system. *Circ Res* 2004; **95:** 210–216.
14. Kishi T, Hirooka Y, Kimura Y, Ito K, Shimokawa H, Takeshita A. Increased reactive oxygen species in rostral ventrolateral medulla contribute to neural mechanisms of hypertension in stroke-prone spontaneously hypertensive rats. *Circulation* 2004; **109:** 2357–2362.
15. Ohtsuki T, Matsumoto M, Suzuki K, Taniguchi N, Kamada T. Mitochondrial lipid peroxidation and superoxide dismutase in rat hypertensive target organs. *Am J Physiol Heart Circ Physiol* 1995; **268:** H1418–H1421.
16. Kimoto-Kinoshita S, Nishida S, Tomura TT. Age-related change of antioxidant capacities in the cerebral cortex and hippocampus of stroke-prone spontaneously hypertensive rats. *Neurosci Lett* 1999; **273:** 41–44.
17. Rikans LE, Hornbrook KR. Lipid peroxidation, antioxidant protection and aging. *Biochim Biophys Acta* 1997; **1362:** 116–127.
18. Sano H, Matsumoto K, Utsumi H. Synthesis and imaging of blood-brain-barrier permeable nitroxyl-probes for free radical reactions in brain of living mice. *Biochem Mol Biol Int* 1997; **42:** 641–647.
19. Tai MH, Wang LL, Wu KL, Chan JY. Increased superoxide anion in rostral ventrolateral medulla contributes to hypertension in spontaneously hypertensive rats via interactions with nitric oxide. *Free Radic Biol Med* 2005; **38:** 450–462.
20. Chan SHH, Tai MH, Li CY, Chan JYH. Reduction in molecular synthesis or enzyme activity of superoxide dismutase and catalase contributes to oxidative stress and neurogenic hypertension in spon-

taneously hypertensive rats. *Free Radic Biol Med* 2006; **40:** 2028–2039.
21. Oliveira-Sales EB, Dugaich AP, Carillo BA, Abreu NP, Boim MA, Martins PJ, et al. Oxidative stress contributes to renovascular hypertension. *Am J Hypertens* 2008; **21:** 98–104.
22. Oliveira-Sales EB, Nishi EE, Carillo BA, Boim MA, Dolnikoff MS, Bergamaschi CT, et al. Oxidative stress in the sympathetic premotor neurons contributes to sympathetic activation in renovascular hypertension. *Am J Hypertens* 2009; **22:** 484–492.
23. Lassegue B, Clempus RE. Vascular NAD(P)H oxidases: Specific features, expression, and regulation. *Am J Physiol Regul Integr Comp Physiol* 2003; **285:** R277–R297.
24. Wang G, Anrather J, Huang J, Speth RC, Pickel VM, Iadecola C. NADPH oxidase contributes angiotensin signaling in the nucleus tractus solitarius. *J Neorosci* 2004; **24:** 5516–5524.
25. Wang G, Anrather J, Glass MJ, Tarsitano J, Zhou P, Frys KA, et al. Nox2, Ca^{2+}, and protein kinase C play a role in angiotensin II-induced free radical production in nucleus tractus solitarius. *Hypertension* 2006; **48:** 482–489.
26. Zimmerman MC, Dunlay RP, Larzartigues E, Zhang Y, Sharma RV, Engelhardt JF, et al. Requirement for Rac1-dependent NADPH oxidase in the cardiovascular and dipsogenic actions of angiotensin II in the brain. *Circ Res* 2004; **95:** 532–539.
27. Sagara Y, Hirooka Y, Kimura Y, Nozoe M, Sunagawa K. Increased reactive oxygen species via Rac1-dependent pathway in rostral ventrolateral medulla contribute to neural mechanisms of hypertension in stroke-prone spontaneously hypertensive rats. *Circulation* 2005; **112**(Suppl II)**:** II-154.
28. Nozoe M, Hirooka Y, Koga Y, Sagara Y, Kishi T, Engelhardt JF, et al. Inhibition of Rac1-derived reactive oxygen species in nucleus tractus solitarius decreases blood pressure and heart rate in stroke-prone spontaneously hypertensive rats. *Hypertension* 2007; **50:** 62–68.
29. Nozoe M, Hirooka Y, Koga Y, Araki S, Konno S, Kishi T, et al. Mitochondria-derived reactive oxygen species mediate sympathoexcitation induced by angiotensin II in the rostral ventrolateral medulla. *J Hypertens* 2008; **26:** 2176–2184.
30. Chan SHH, Wu KLH, Chang AYW, Tai MH, Chan JYH. Oxidative impairment of mitochondrial electron transport chain complexes in rostral ventrolateral medulla contributes to neurogenic hypertension. *Hypertension* 2009; **53:** 217–227.
31. Zimmerman MC, Zucker IH. Mitochondrial dysfunction and mitochondrial-produced reactive oxygen species: New targets for neurogenic hypertension? *Hypertension* 2009; **53:** 112–114.
32. Kimura Y, Hirooka Y, Sagara Y, Ito K, Kishi T, Shimokawa H, et al. Overexpression of inducible nitric oxide synthase in rostral ventrolateral medulla causes hypertension and sympathoexcitation via an increase in oxidative stress. *Circ Res* 2005; **96:** 252–260.
33. Kimura Y, Hirooka Y, Kishi T, Ito K, Sagara Y, Sunagawa K. Role of inducible nitric oxide synthase in rostral ventrolateral medulla in blood pressure regulation in spontaneously hypertensive rats. *Clin Exp Hypertens* 2009; **31:** 281–286.
34. Zimmerman MC, Sharma RV, Davisson RL. Superoxide mediates angiotensin II-induced influx of extracellular calcium in neural cells. *Hypertension* 2005; **45:** 717–723.
35. Sun C, Sellers KW, Sumners C, Raizada MK. NAD(P)H oxidase inhibition attenuates neuronal chronotropic actions of angiotensin II. *Circ Res* 2005; **96:** 659–666.
36. Chan SHH, Hsu KS, Hunag CC, Wang LL, Ou CC, Chan JYH. NADPH oxidase-derived superoxide anion mediates angiotensin II-induced pressor effect via activation of p38 mitogen-activated protein kinase in the rostral ventrolateral medulla. *Circ Res* 2005; **97:** 772–780.
37. Kishi T, Hirooka Y, Konno S, Ogawa K, Sunagawa K. Angiotensin II type 1 receptor-activated caspase-3 through Ras/mitogen-activated protein kinase/extracellular signal-regulated kinase in the rostral ventrolateral medulla is involved in sympathoexcitation in stroke-prone spontaneously hypertensive rats. *Hypertension* 2010; **55:** 291–297.
38. Reja V, Goodchild AK, Phillips JK, Pilowsky PM. Upregulation of angiotensin AT1 receptor and intracellular kinase gene expression in hypertensive rats. *Clin Exp Pharmacol Physiol* 2006; **33:** 690–695.
39. McKinley MJ, Albiston AL, Allen AM, Mathai M, May CN, McAllen RM, et al. The brain renin-angiotensin system: Location and physiological roles. *Int J Biochem Cell Biol* 2003; **35:** 901–918.
40. Dampney RAL, Fontes MAP, Hirooka Y, Potts PD, Tagawa T. Role of angiotensin II receptors in the regulation of vasomotor neurons in the rostral ventrolateral medulla. *Clin Exp Pharmacol Physiol* 2002; **29:** 467–472.
41. Wang JM, Tan J, Leenen FHH. Central nervous system blockade by peripheral administration of AT1 receptor blockers. *J Cardiovasc Pharmacol* 2003; **41:** 593–599.
42. Culman J, Blume A, Gohlke P, Unger T. The renin-angiotensin system in the brain: Possible therapeutic implications for AT1-receptor blockers. *J Hum Hypertens* 2002; **16:** S64–S70.
43. Gohlke P, Weiss S, Jansen A, Wienen W, Stangier J, Rascher W, et al. AT1 receptor antagonist telemisartan administered peripherally inhibits central responses to angiotensin II in conscious rats. *J Pharmacol Exp Ther* 2001; **298:** 62–70.
44. Nishimura Y, Ito T, Hoe KL, Saavedra JM. Chronic peripheral administration of the angiotensin II AT1 receptor antagonist candesartan blocks brain AT1 receptors. *Brain Res* 2000; **871:** 29–38.
45. Sagara Y, Ito K, Kimura Y, Hirooka Y. Telmisartan reduces oxidative stress in the brain with sympathoinhibitory effects in stroke-prone spontaneously hypertensive rats. *Circulation* 2004; **110**(Suppl III)**:** 265.
46. Yang CY, Lin MT. Oxidative stress in rats with heatstroke-induced cerebral ischemia. *Stroke* 2002; **33:** 790–794.
47. Sagara Y, Hirooka Y, Nozoe M, Koga Y, Sunagawa K. Contribution of angiotensin II in the increased reactive oxygen species in rostral ventrolateral medulla and enhanced central sympathetic outflow in stroke-prone spontaneously hypertensive rats. *Circulation* 2006; **114**(Suppl II)**:** 271.
48. Araki S, Hirooka Y, Kishi T, Yasukawa K, Utsumi H, Sunagawa K. Olmesartan reduces oxidative stress in the brain of stroke-prone spontaneously hypertensive rats assessed by an in vivo ESR method. *Hypertens Res* 2009; **32:** 1091–1096.
49. Sano H, Naruse M, Matsumoto K, Oi T, Utsumi H. A new nitroxyl-probe with high retention in the brain and its application for brain imaging. *Free Radic Biol Med* 2000; **28:** 959–969.
50. Lin Y, Matsumura K, Kagiyama S, Fukuhara M, Fujii K, Iida M. Chronic administration of olmesartan attenuates the exaggerated pressor response to glutamate in the rostral ventrolateral medulla of SHR. *Brain Res* 2005; **1058:** 161–166.
51. Pelisch N, Hosomi N, Ueno M, Masugata H, Murao K, Hitomi H, et al. Systemic candesartan reduces brain angiotensin II via down-regulation of brain renin-angiotensin system. *Hypertens Res* 2010; **33:** 161–164.
52. Mogi M, Horiuchi M. Remote control of brain angiotensin II levels by angiotensin receptor blockers. *Hypertens Res* 2010; **33:** 116–117.
53. Konno S, Hirooka Y, Araki S, Koga Y, Kishi T, Sunagawa K. Azelnidipine decreases sympathetic nerve activity via antioxidant effect in the rostral ventrolateral medulla of stroke-prone spontaneously hypertensive rats. *J Cardiovasc Pharmacol* 2008; **52:** 555–560.
54. Hirooka Y, Kimura Y, Nozoe M, Sagara Y, Ito K, Sunagawa K. Amlodipine-induced reduction of oxidative stress in the brain is associated with sympatho-inhibitory effects in stroke-prone spontaneously hypertensive rats. *Hypertens Res* 2006; **29:** 49–56.
55. Kimura Y, Hirooka Y, Sagara Y, Sunagawa K. Long-acting calcium channel blocker, azelnidipine, increases endothelial nitric oxide synthase in the brain and inhibits sympathetic nerve activity. *Clin Exp Hypertens* 2007; **29:** 13–21.
56. Sakai K, Hirooka Y, Matsuo I, Eshima K, Shigematsu H, Shimokawa H, et al. Overexpression of eNOS in NTS causes hypotension and bradycardia in vivo. *Hypertension* 2000; **36:** 1023–1028.
57. Kishi T, Hirooka Y, Sakai K, Shigematsu H, Shimokawa H, Takeshita A. Overexpression of eNOS in the RVLM causes hypotension and bradycardia via GABA release. *Hypertension* 2001; **38:** 896–901.
58. Kishi T, Hirooka Y, Ito K, Sakai K, Shimokawa H, Takeshita A. Cardiovascular effects of endothelial nitric oxide synthase in the rostral ventrolateral medulla in stroke-prone spontaneously hypertensive rats. *Hypertension* 2002; **39:** 264–268.
59. Kishi T, Hirooka Y, Kimura Y, Sakai K, Ito K, Shimokawa H, et al. Overexpression of eNOS in RVLM improves impaired baroreflex control of heart rate in SHRSP. *Hypertension* 2003; **41:** 255–260.
60. Kishi T, Hirooka Y, Shimokawa H, Takeshita A, Sunagawa K. Atorvastatin reduces oxidative stress in the rostral ventrolateral medulla of stroke-prone spontaneously hypertensive rats. *Clin Exp Hypertens* 2008; **30:** 1–9.
61. Kishi T, Hirooka Y, Konno S, Sunagawa K. Sympathoinhibition induced by centrally administered atorvastatin is associated with alteration of NAD(P)H and Mn superoxide dismutase activity in rostral ventrolateral medulla of stoke-prone spontaneously hyper-